



**National Technical University of Athens**

School of Mechanical Engineering

Department of Mechanical Design & Automatic Control

Machine Design Laboratory

Diploma Thesis

**Optimal design and simulation of a planetary gear transmission of a rotary peristaltic pump for drug delivery in the presence of misalignments**

Kleanthis Ragkousis

Supervisor: V.Spitas, Associate Professor

Athens, October 2022



## **Εθνικό Μετσόβιο Πολυτεχνείο**

**Σχολή Μηχανολόγων Μηχανικών**

**Τομέας Μηχανολογικών Κατασκευών & Αυτομάτου Ελέγχου**

**Εργαστήριο Στοιχείων Μηχανών**

### **Διπλωματική Εργασία**

**Βέλτιστος σχεδιασμός και προσομοίωση λειτουργίας πλανητικού συστήματος μετάδοσης κίνησης περιστροφικής περισταλτικής αντλίας παρουσία σφαλμάτων τοποθέτησης**

**Κλεάνθης Ραγκούσης**

Επιβλέπων: Β. Σπιτάς, Αναπληρωτής Καθηγητής

Αθήνα, Οκτώβριος 2022

---



## Ευχαριστίες

Στο σημείο αυτό θα ήθελα να ευχαριστήσω ορισμένα άτομα τα οποία είχαν καθοριστικό ρόλο, στην ολοκλήρωση της διπλωματικής μου εργασίας όπως και των σπουδών μου στη Σχολή Μηχανολόγων Μηχανικών. Αρχικά θα ήθελα να ευχαριστήσω θερμά, τον επιβλέποντα της εργασίας, Αναπληρωτή Καθηγητή Σπιτά, καθώς μου ανέθεσε ένα τόσο ενδιαφέρον και σύγχρονο θέμα, ενώ παράλληλα βρισκόταν πάντα δίπλα μου για να απαντήσει σε κάθε απορία που πρόκυπτε και για την υπομονή που επέδειξε και σε αυτή αλλά και σε κάθε άλλη εργασία μου στη σχολή. Φυσικά δε θα μπορούσα να παραλείψω το να ευχαριστήσω θερμά τους υποψήφιους διδάκτορες Νίκο Ρόγκα και Χρίστο Καλλίγερο . Χωρίς την καθοδήγηση και την βοήθεια τους επί των τεχνικών ζητημάτων που προέκυπταν, όπως και τις συμβουλές τους, η παρούσα εργασία δεν θα μπορούσε να υλοποιηθεί.

Επίσης θα ήθελα να ευχαριστήσω τους γονείς μου και τα αδέρφια μου και τη γιαγιά μου για την υπομονή και την αμέριστη υποστήριξη τους που έδειξαν σε όλα τα φοιτητικά και μαθητικά μου χρόνια.

Με την παρούσα διπλωματική ολοκληρώνω τις σπουδές μου στη Σχολή των Μηχανολόγων Μηχανικών του Ε.Μ.Π. και το χρωστάω στους φίλους μου που μου συμπαραστάθηκαν όλα αυτά τα χρόνια είτε σε εργασίες μέσα στη σχολή είτε αφιερώνοντας το χρόνο τους με πολύωρες συζητήσεις περί αυτής. Πιο συγκεκριμένα θα ήθελα να ευχαριστήσω τους στενούς μου φίλους Παρασκευά Σκιαδόπουλου και Κωνσταντίνο Παπαγιαννόπουλο για τη συνεχή τους υποστήριξη και τέλος τους στενούς μου φίλους και συνεργάτες μέσα από τη σχολή: Ιωάννη Πυροβολάκη, Ιάκωβο Κρητικό και Αθανασία Ζουμπάκη και Βασιλική Ηλιοπούλου.

## Abstract

The goal of this thesis is to design gear profiles that have a better behavior in the presence of misalignments as well as to model through Finite Element Analysis the planetary system of a roller pump. The design of the gears is achieved using MATLAB and KISSOFT for the development of the profiles and then SOLIDWORKS for the CAD model. The modelling of the planetary gear train is achieved via the implementation of the commercial software ANSYS Workbench. The process begins with the theoretical background of the Hertzian Theory of contact for an aligned and misaligned pair of gears. Afterwards based on the theory of planetary systems for the kinematic analysis and for the contact stresses as well as the decoupling of the systems. The overview of the mechanical phenomena is complete and allowing the further study using FEA.

For the extraction of the results for the planetary system and the roller-pump-carrier system as well as the verification of the code ANSYS Workbench was implemented. The one-stage gear pairs were tested in static analysis with three different profiles (involute, modified involute, given profile). The involute profile was used most of the time both for the planar and for the misaligned tests as a benchmark in order to have a point of reference that the analysis is working correctly and follow the conjectures for plastic gears. Completing the one-stage pairs it was necessary for the Planetary Gear Train to be tested in static analysis to verify the workability of the modified profiles in the application. The static analysis of the gear systems gave a better understanding of the pressures that develop during contact. However, it was deemed necessary to check the Planetary Gear Train in transient analysis as well. This was done in order to determine the effect of both the misalignments and the roller pump as a whole.

Furthermore, a kinematic analysis as a rigid body motion was done using Motion Analysis in SOLIDWORKS, in order to determine the trajectories of both the planets-rollers and the sun-roller of the whole system as a control for the transient analysis of the roller-pump-carrier system in ANSYS.

Finally, the roller-pump-carrier system was modelled in a transient analysis in ANSYS to see the effects of plastic rollers on the compression of the tube in a deep occlusion model, as well as how the real model moves due to the loose fit of the planets on the carrier.

## Περίληψη

Στόχος αυτής της διπλωματικής εργασίας είναι ο σχεδιασμός προφίλ οδοντωτών τροχών που έχουν καλύτερη συμπεριφορά παρουσία απευθυγραμμίσεων καθώς και η μοντελοποίηση μέσω της Ανάλυσης Πεπερασμένων Στοιχείων του πλανητικού συστήματος μιας περισταλτικής αντλίας. Ο σχεδιασμός των οδοντωτών τροχών επιτυγχάνεται με χρήση των λογισμικών MATLAB και KISSSOFT για την ανάπτυξη των προφίλ και στη συνέχεια η χρήση του λογισμικού SOLIDWORKS για το τρισδιάστατο μοντέλο. Η μοντελοποίηση του πλανητικού συστήματος επιτυγχάνεται μέσω της εφαρμογής του εμπορικού λογισμικού ANSYS Workbench. Η διαδικασία αναλύει με το θεωρητικό υπόβαθρο της Θεωρίας του Χερτς της επαφής για ένα ευθυγραμμισμένο και κακώς ευθυγραμμισμένο ζεύγος οδοντωτών τροχών. Στη συνέχεια με βάση τη θεωρία των πλανητικών συστημάτων για την κινηματική ανάλυση και για τις τάσεις επαφής καθώς και την αποσύνδεση των συστημάτων του πλανητικού συστήματος και του συστήματος της περισταλτικής αντλίας. Με την επισκόπηση των μηχανικών φαινομένων να είναι πλήρης μπορεί να γίνει περαιτέρω μελέτη με χρήση πεπερασμένων στοιχείων.

Για την εξαγωγή των αποτελεσμάτων για το πλανητικό σύστημα και το σύστημα ραούλων-αντλίας-φορέα καθώς και η επαλήθευση του κωδικού ANSYS Workbench. Τα ζεύγη ταχυτήτων ενός σταδίου δοκιμάστηκαν σε στατική ανάλυση με τρία διαφορετικά προφίλ (εξειλιγμένη, τροποποιημένη εξειλιγμένη, δεδομένο προφίλ). Το προφίλ της εξειλιγμένης χρησιμοποιήθηκε τις περισσότερες φορές τόσο για τις επίπεδες όσο και για τις δοκιμές με απευθυγραμμίσεις ως σημείο αναφοράς προκειμένου να βεβαιωθεί ότι η ανάλυση λειτουργεί σωστά και ότι ακολουθεί τις εικασίες για τους πλαστικούς οδοντωτούς τροχούς. Ολοκληρώνοντας τα ζεύγη των οδοντωτών τροχών ήταν απαραίτητο και το πλανητικό σύστημα να δοκιμαστεί σε στατική ανάλυση για να επαληθευτεί η λειτουργικότητα των τροποποιημένων προφίλ στην εφαρμογή. Η στατική ανάλυση των συστημάτων γραναζιών έδωσε μια καλύτερη κατανόηση των πιέσεων που αναπτύσσονται κατά την επαφή. Ωστόσο, κρίθηκε απαραίτητος ο έλεγχος του πλανητικού συστήματος και σε μη μόνιμη ανάλυση. Αυτό έγινε για να προσδιοριστεί η επίδραση τόσο των λανθασμένων ευθυγραμμίσεων όσο και της επίδρασης της αντλίας στο πλανητικό σύστημα ως σύνολο.

Επιπλέον, έγινε κινηματική ανάλυση ως ανάλυση κίνησης άκαμπτου σώματος χρησιμοποιώντας την Ανάλυση Κίνησης στο SOLIDWORKS, προκειμένου να προσδιοριστούν οι τροχιές τόσο των πλανητών-ραούλων όσο και του ραούλου του ήλιου ολόκληρου του συστήματος ως έλεγχος για τη μη μόνιμη ανάλυση του συστήματος ραούλων-αντλίας-φορέα στο ANSYS.

Τέλος, το σύστημα ραούλων-αντλίας-φορέας μοντελοποιήθηκε σε μια μη μόνιμη ανάλυση στο ANSYS για να εξαχθούν τα αποτελέσματα των πλαστικών κυλίνδρων στη συμπίεση του σωλήνα

σε ένα μοντέλο βαθιάς απόφραξης, καθώς και πώς κινείται το πραγματικό μοντέλο λόγω της χαλαρής προσαρμογής του οι πλανήτες στον φορέα.

## Contents

Ευχαριστίες .....	3
Abstract .....	4
Περίληψη .....	5
1. Introduction-Theoretical Background.....	11
1.1 Peristaltic Pumps. Functionality and Characteristics .....	11
1.1.1 Basic operation of peristaltic pumps .....	11
1.1.2. Types of Peristaltic Pumps .....	11
1.1.3 Advantages and Disadvantages .....	13
1.1.4 Current Model.....	15
1.2 Epicyclic gear train .....	17
1.3 Plastic Gears .....	18
1.3.1 Abrasive advances.....	18
1.3.2 Gear Design Advances on Many Fronts .....	18
1.4 Crowning .....	19
2. Design for optimal gear profiles .....	20
2.1 Constraints and design of undercuts .....	20
2.1.1 Basic Law of gear theory of involution.....	21
2.1.2 Geometrical Constraints during profile designing .....	24
2.1.3 Form Optimization with respect to Misalignments .....	28
2.2 CAD of the Modified Profiles .....	32
2.2.1 Design Trials .....	32
2.2.2 Gear assemblies using KISSSOFT and SOLIDWORKS .....	35
3. Overview of the mechanical phenomena .....	39
3.1 Contact Theory with and without Misalignments in one-stage pair of gears .....	39
3.2 Contact Theory of a PGT .....	43
3.3 Kinematic analysis of PGT and the system and simplification of the model .....	44
3.3.1 Decoupling of the system .....	44
3.3.2 Kinematic analysis of a PGT .....	45
3.3.3 Modelling of the system in SOLIDWORKS.....	48
4. FEM Analysis in Ansys Workbench .....	50
4.1. Three-dimensional modelling of involute spur gears .....	50



---

4.1.1 Static Analysis of the cylindrical gear pair and the PGT .....	51
4.1.2 Transient Analysis of the PGT .....	59
4.2 Modelling of the RPC system .....	61
4.2.1 Transient analysis.....	62
5. Results.....	65
5.1. Analysis of cylindrical gear pair and PGT .....	65
5.1.1 Static Structural Analysis.....	65
5.1.2 Comparison of the one-stage gear pairs.....	83
5.1.3 PGT test with Modified Involute Profile with 2° misalignment along the Y axis .....	86
5.1.4 PGT test with Given Profile with 2° misalignment along the Y axis.....	87
5.1.5 Comparison of the PGT systems .....	88
5.1.6 Transient of the PGT .....	88
5.2 Analysis of the RPC system .....	90
5.2.1 Transient Analysis of the Roller-pump-carrier system.....	90
6. Conclusion.....	94
7. References .....	95

---

Figure 1 Peristaltic Pump flow scheme .....	11
Figure 2 Principle of operation of a roller pump .....	14
Figure 3 Current Model of the Peristaltic Pump .....	15
Figure 4 Fit of the planet and the carrier .....	16
Figure 5 Misaligned Planet due to compression .....	16
Figure 6 3D printed Planetary Gear Train .....	17
Figure 7 Involute Barreling $C\alpha$ , lead $C\beta$ and lead slope $CH\beta$ .....	20
Figure 8 Condition of no penetration .....	21
Figure 9 Condition of steady transmission ratio .....	22
Figure 10 Different positions of point K to define angle $\theta$ .....	24
Figure 11 Curvature for point G .....	27
Figure 12 Avoidance of double contact points .....	27
Figure 13 Error along X axis .....	28
Figure 14 Error along Y axis .....	28
Figure 15 Differentiation due to errors .....	29
Figure 16 Overlapping X and Z error .....	30
Figure 17 Differentiation of speed .....	31
Figure 18 Final theoretical Result .....	32
Figure 19 1st Test .....	33
Figure 20 Involute profile $m=1.5$ .....	35
Figure 21 Tangent Involute Profiles .....	37
Figure 22 Scanning of the tooth facewidth .....	38
Figure 23 Basic Gear geometry .....	40
Figure 24 Gear Misalignment (a) axial (b) angular .....	42
Figure 25 The load distribution of gear surface (a) aligned (b) misaligned .....	43
Figure 26 Involute profile and tooth-to-tooth contact .....	44
Figure 27 Structure and schematic diagram of a planetary gear train .....	45
Figure 28 Superposition of motions .....	47
Figure 29 Velocity distribution on the rotating planet gear with moving carrier .....	48
Figure 30 Model of the pump in Motion analysis .....	49
Figure 31 Trajectories of the planets and the sun .....	50
Figure 32 Cylindrical Bodies in DM .....	52
Figure 33 Contact Parameters .....	53
Figure 34 Final contact regions .....	54
Figure 35 Deformation of a linear element under pure bending .....	55
Figure 36 Deformation of a quadratic element under pure bending .....	55
Figure 37 Contact between second order elements .....	56
Figure 38 Final Mesh .....	57
Figure 39 Meshing of the PGT in transient analysis .....	61
Figure 40 Frictional contact of the planet-roller with the tube .....	63
Figure 41 Initial and boundary conditions for the RPC .....	64
Figure 42 Frontal view of deformation .....	66
Figure 43 Equivalent von-Mises Stress frontal .....	67

---

Figure 44 Deformation of the driver gear .....	68
Figure 45 Deformation of the driven gear .....	69
Figure 46 Equivalent von Mises stress of the driver gear .....	70
Figure 47 Equivalent von Mises stress of the driven gear .....	70
Figure 48 Energy consumption for tight fit .....	91
Figure 49 Energy consumption for loose fit .....	91
Figure 50 Rollers movement .....	92
Figure 51 Elastic Strain of deep occlusion .....	93
Figure 52 Energy consumption of deep occlusion .....	93

## 1. Introduction-Theoretical Background

### 1.1 Peristaltic Pumps. Functionality and Characteristics

#### 1.1.1 Basic operation of peristaltic pumps

In this section the operation of peristaltic pumps will be discussed for the most used two rolled tube pump. However, this operation differs somehow for some of the pumps discussed in the rest of the paper.

At the beginning of the sequence the first roller closes the tubing inlet. As a result, the roller moves forward and pushes the pump segment to the manifold. Hence, it pushes the fluid inside the tube forward and generates a pressure wave. Before reaching the outlet, the other roller closes the tube inlet, and in this way, it prevents the back-flow. After the first roller leaves the outlet, the other roller's task will be to generate the next pressure wave. The described sequence is repeated over time and can be seen in Fig. 1.

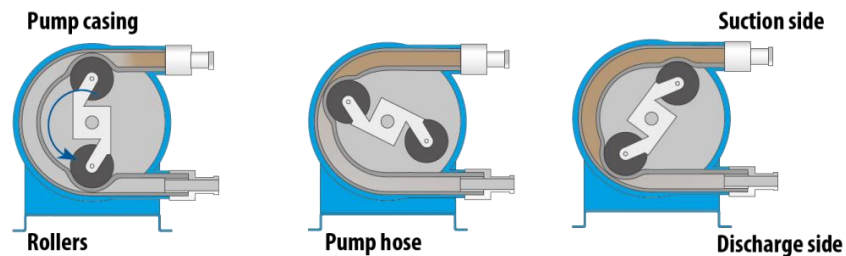


Figure 1 Peristaltic Pump flow scheme

#### 1.1.2. Types of Peristaltic Pumps

Peristaltic pumps can be distinguished by many points. One of the most important differences can be characterized by tubing. From this aspect two types can be distinguished: the tube pumps and the hose pumps. The difference between them is the hose pumps contain a pump segment, which is a reinforced tube, called hose. These hoses are harder to be pressed and this way they need bigger and stronger motors for the same flow; hence, they are more expensive to operate. The main advantage of hose pumps is that they can operate against much higher pressure than tube pumps working up to 16 bars.

The tube pumps contain silicon, PVC, fluoropolymer, or other polymer as material of tubing. These are the most common type of peristaltic pumps tubing and as materials are improving the difference between hose pumps and tube pumps are melting. Tube pumps can operate against less pressure, but they need smaller motors and force to operate; hence, this way they are space-saving and cheaper to work with [1].

Comparing to other pumps the (linear) peristaltic pump is more accurate, when the pressure gradient is under  $-13.3 \text{ Pa}$  ( $-100 \text{ mmHg}$ ). In other cases, piston pump is more accurate.

The next difference between peristaltic pumps can be the type of propulsion. The most current type contains a central rotor and on these rotors, it has rollers. The task of these rollers is to press the lining and by this way to force the transport, but also to prevent the back-flow.

There is a solution, which only needs one rotor to operate with. This 360-degree peristaltic pump is a rarity, common pumps contain at least two rollers. On some occasion one of the rollers roles could be only to prevent back-flow, but usually the entire rollers task is to force the fluid movement.

With increased number of rollers, it is possible to generate more pressure waves over time and this way to decrease the deviance of pressure on the output. However, this means more occlusion for the same transferred volume; hence, it reduces the lifetime of lining.

The pumps can be distinguished by how their rollers are fixed. The simplest solution is the fixed occlusion. The rollers have fixed locus; hence, they keep the same distance from the manifold during the entire rotation(s). This method is simple, robust and undemanding. However, fixed occlusion reduces the lifetime of the tube segment because it depends on its wall thickness.

Alternatively, the rollers can be spring loaded. In this case the rollers are mounted on springs, and this way the rollers keep almost constant pressure on the tubing. The advantage of using spring loaded rollers is the elevated tubing lifetime, the constant pressure and that they can handle a broader range of wall thickness. The shape of the rotor and the housing is usually symmetric; however, there are solutions, where the asymmetry of the system is used to increase lifetime and stability.

Above, the rotor type peristaltic pumps were discussed, but it is not possible to transport fluid in circular tubing, where there could be linear pumps as well. These linear pumps are often called "finger pumps". In linear peristaltic pumps cams generate the necessary pressure and also cams prevent the back-flow. The name finger pump shows well how they work. The cams close each other one-by-one; hence, pushing the fluid forward. After this the cams release the lining. At the other end of the pump before the last cam release the tube segment the first cam closes again, and this way the pressure is kept and back-flow is prohibited. This process is called peristalsis and is used in many biological systems such as the gastrointestinal tract.

The advantage of linear peristaltic pumps is they are space-saving, but on the other hand they need more complex mechanics.

### 1.1.3 Advantages and Disadvantages

Advantages of peristaltic pumps can be summarized as follows.

As the transported fluid flows in the tubing and the driving force is generated by the compression the fluid will not get contaminated, neither the pump head nor the pump mechanism. It is appropriate to use only clean tubing, and the pump mechanism does not need any cleaning. Hence, it is easy to keep them clean and sanitized. As the fluid does not leave the tubing these pumps are virtually immune to abrasive media and many chemicals. Some of the tubing material can be autoclaved; consequently, sterility can be kept.

Peristaltic pumps do not need any specific action for priming as they are capable of self-priming. They are also insensitive to dry running as the fluid is not necessary as lubricant and the tubing does not damage if compressed empty. Moreover, pumps do not contain any valves, seals or glands; hence, they are easy and cheap to maintain and the chance of malfunction is also lower.

They can operate reversibly against other type of pumps. Furthermore, during the use mostly the tube is worn by time, which is cheap to replace. Multi-channel systems can be built easily as well.

Their suction height is excellent and when stopped, no siphoning effect will occur. The viscosity of the fluid does not influence the transport; hence, suspensions and sludges cannot influence the transport.

The delivery is gentle due to the low shearing forces; by this way they are ideal for shear-sensitive fluids such as blood (due to the blood cells). Moreover, their high repeatability makes them suitable for auto-analyzers.

However, disadvantages of peristaltic pumps can be formulated as well:

Due to deviation caused through the production and the replaceable tubing, the pump system must be calibrated to reach acceptable accuracy. Due to the wear the tubing it needs to be changed and recalibrated over time. In case of extensive use or in absence of exchange the tube may leak. In some case their chemical inertness can be disadvantage as well.

Slight pulsation is inevitable at work. The flow rate is sensitive to varying differential pressure conditions and their maximal differential pressure is lower comparison to gear and piston pumps, as shown in figure 2.

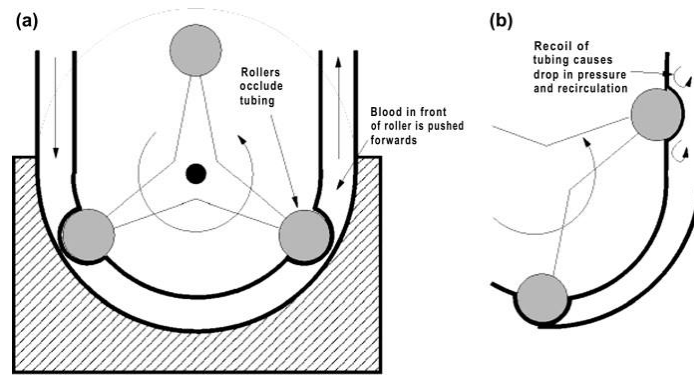


Figure 2 Principle of operation of a roller pump

Peristaltic pumps can be found in many applications. Below a review can be found with the practical property which is necessary in the given application.

By the utilization of the minimal shearing forces we could have:

- Hemodialysis machines
- Open-heart bypass pump machines
- Beverage dispensing

By the utilization that they are capable to deliver both suspensions and sludges we can distinguish:

- Concrete pump
- Sewage sludge
- Pulp and paper plants

Regarding if one would like to help that fluid does not get contaminated we could have:

- Medical infusion pump
- Pharmaceutical production
- Chemical analytical equipments

From high repeatability point of view:

- Autoanalyzers

Regarding the chemical compatibility there is:

- Carbon monoxide monitor
- Dosing systems
- Calcium reactors

Regarding the space spare solution, one should consider:

- Mobile peritoneal dialysis pump .

There are three materials currently used for tubing in the medical device industry: silicone; latex and polyvinyl chloride (PVC). Regarding microparticle releasing, the PVC is the best material for tubing because the latex generates more hemolysis and the silicon tube releases more microparticles than the PVC. One of the common problems in blood pumps is the tube occlusion. Occlusion can be controlled by either increasing or decreasing the compression of the tube by the rollers and the optimization between increasing and decreasing the compression is very vital in pumping the blood, because more compression increases hemolysis and less generates occlusion, although the priority is with forward output of the blood.

#### 1.1.4 Current Model

In this thesis the peristaltic pump that is studied is shown in figure 3. This pump differs from the typical pumps because of the existence of greater misalignments than in most cases.

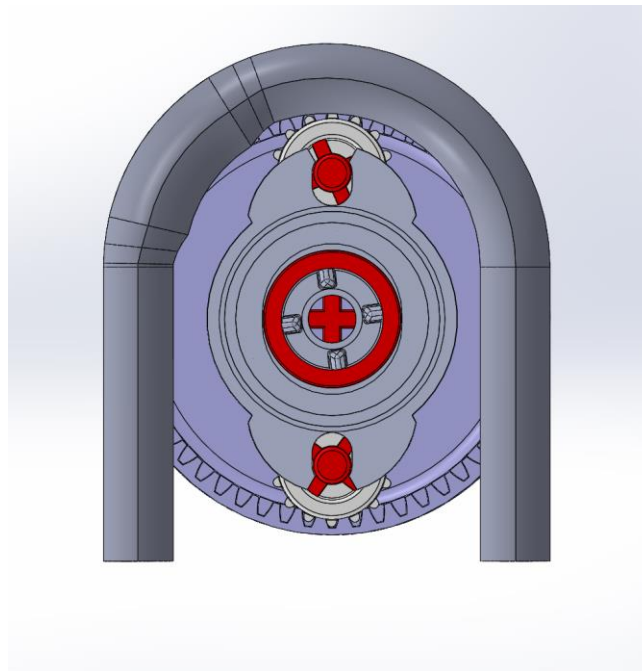


*Figure 3 Current Model of the Peristaltic Pump*



Those misalignments are caused by the loose fit of the rollers that are used to press on the tube as shown in Figure 4.

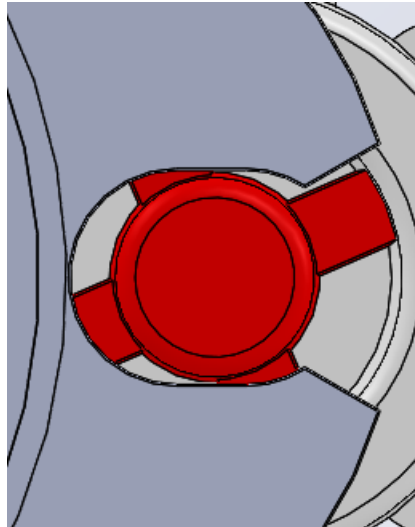


*Figure 4 Fit of the planet and the carrier*

The rollers deform the tube and are designed make a  $2^\circ$  angle relative to the vertical axes of the planetary system that is used to rotate the rollers, as shown in figure 5. Those misalignments greatly affect the performance and the efficiency of the of the PGT and cause extra noise and disruption of the flow rate.

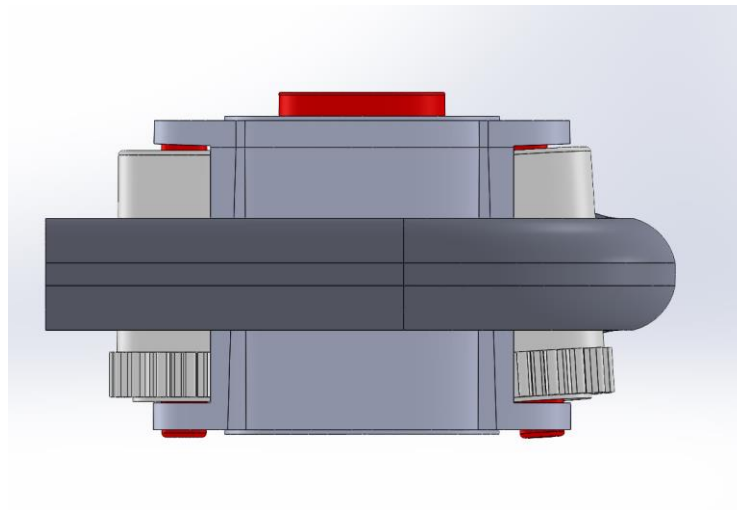


*Figure 5 Misaligned Planet due to compression*

## 1.2 Epicyclic gear train

An epicyclic gear train (also known as a planetary gearset) consists of two central geared members mounted so that the center of one member revolves around the center of the other. The inner central member is named as “sun gear” whereas the outer central member which is an internal gear is called “ring (annulus) gear”. A carrier connects the centers of the two gears and rotates the planet and sun gears mesh so that their pitch circles roll without slip. A point on the pitch circle of the planet gear traces an epicycloid curve. In this simplified case, the sun gear is fixed and the planetary gear(s) roll around the sun gear.

An epicyclic gear train can be assembled so the planet gear rolls on the inside of the pitch circle of a fixed, outer gear ring, or ring gear. In this case, the curve traced by a point on the pitch circle of the planet is a hypocycloid.



*Figure 6 3D printed Planetary Gear Train*

The combination of epicycle gear trains with a planet engaging both a sun gear and a ring gear is called a planetary gear train (PGT). In the case of this thesis, the ring gear is fixed and the sun gear is driven. The mechanics that govern a PGT will be analyzed thoroughly.

### 1.3 Plastic Gears

Plastic gears have a long history in autos, appliances, office equipment, tools, medical equipment industries. Designers continue to extend their use in transferring torque and motion as polymers improve and processing gains in sophistication. They often choose plastic for gears over metal because of the many benefits plastic offers.

#### 1.3.1 Abrasive advances

Plastic provides great design freedom, allowing for gear configurations too difficult or expensive to create in metal, such as cluster gears, in which more than one gear is created in a single molded part. Plastic gears also offer good loading properties, relatively low noise, excellent wearability and lubricity, and good chemical and thermal resistance.

A growing preference for plastic gears is evident in the industry, where electrical systems are eliminating hydraulics and cables in both interior and exterior applications. These systems depend on plastic gears for the smooth and quiet operation of lift gates, tracking headlights, window movements, under hood electronic throttle body controls, and much more.

Plastic gears are also preferred in the medical industry due to their dimensional stability across a wide temperature range, as well as for their chemical resistance and processability.

Cost alone is a strong motivator for selecting plastic. Powdered metal gears often cost about twice as much as a comparable thermoplastic gear. The same gear hobbled from a metal gear blank typically costs three times as much.

#### 1.3.2 Gear Design Advances on Many Fronts

Plastics are primarily used in involute gears, most commonly spur gears. New plastic designs are pushing the boundary on plastic gear size, structure, and geometry in these and other gear types to gain greater power, improved function, and lower cost. In many cases, current plastic gear concepts translate configurations used successfully in metal gears. In others, they involve new approaches specially developed for plastic gears. These approaches include:

- Non-linear gears that have a tailored output. Such gears involve a variety of design methods, including those having eccentric shaft locations and thus varying displacement profiles, elliptical, and other out-of-round gears that cycle through various speeds and torques with each rotation, and gears having step changes in radius so power output shifts suddenly to meet the needs of an application.
- Epicyclic gears, one approach to split power paths, which offer greater power and torque transfer in a relatively small package.
- Herringbone gears, in which two helical directions meet to cancel out axial thrust loads that are typically detrimental to simple helical plastic gears.
- Two-shot molded gears that allow a variety of solutions to common gear issues. Examples of this include gears having a rigid core and a lubricous surface layer or a gear ring and hub of the same polymer separated by a shock-absorbing material.
- Crowned gears have been demonstrated in plastic to help maintain transmission accuracy in transmissions where shaft alignment is less than optimal. One example of this involves lead crowning, where the teeth can be taller, thicker, or both at the center of the gear face in order to overcome poor load distribution due to misalignment.
- Zero- or low-backlash designs that eliminate clearance between gear teeth. Such designs help overcome manufacturing errors and bearing run-out. They also help limit noise in lightly or moderately loaded gears that reverse direction repeatedly.
- Tooth profiles having customized pressure angles on their forward and reverse flanks to enhance efficiency and sliding, tailor bending stress, and reduce heat and noise.

## 1.4 Crowning

Traditional non-modified gear drive is operated under assembly errors, which leads to very serious tooth impact at the tooth replacing point, which causes a high level of gear vibration and noise. Also, ideal spur gears with line contact are very sensitive to axial misalignment and manufacturing errors which cause the edge contact of gear drive. Concentration of contact load at one end of a gear tooth produces bending stress concentration and reduces lifetime of a gear drive. Tooth breakage at one end of a gear associated with misalignment. The light scuff marks towards the end of the teeth also indicates misalignment. The easiest way to avoid the edge contact is to localize the bearing contact by crowning gear tooth surfaces. Further crowning modification is still required to transform the meshing from line contact to point contact. The

most common way of crowning is the so-called lead crowning. The lead crowning of spur gear can be considered as the longitudinal deviation from a straight line along the tooth width. This modification prevents excessive loading at the ends due to misalignment, tooth inaccuracies, deflection, or heat treatment. As the load increases, a smooth spreading of the contact occurs until the entire flank is loaded. There are different forms that can be chosen for the modified tooth profile including linear and parabolic variation. Nowadays, in order to pursue the development of a higher quality of transmission, the former method of using parabolic functions need improvement. The parabolic function demands a shrinking of the tooth face inwards near the top land and fillet, which results in a decrease in bending strength of the tooth fillet. But, for a fourth order polynomial function shrinking near the tooth fillet is smaller and thus the tooth fillet is stronger. An increased magnitude of crowning weakens the pitting durability, and too small crowning decreases the ability to stabilize the bearing contact. Although crowning is a very important manufacturing technique in gearing field, a sufficient analysis for the proper amount of crowning has not been provided. It is preferable to crown the pinion tooth surface than the gear tooth surface since the number of pinion teeth is smaller. The conjugation of crowned pinion tooth surface and an ordinary gear tooth surface should be a subject of special investigation directed at minimization of transmission errors and favorable location of bearing contact [2].

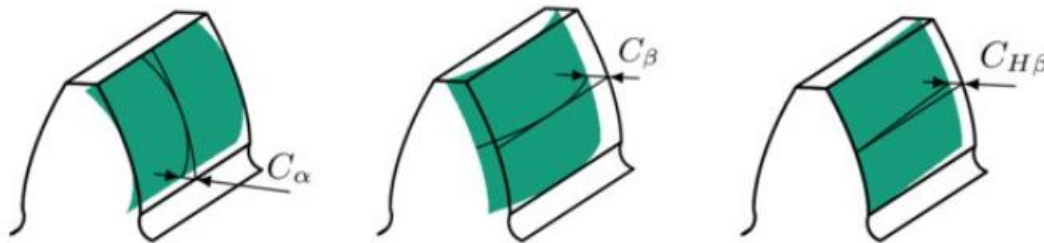


Figure 7 Involute Barreling  $C_\alpha$ , lead  $C_\beta$  and lead slope  $C_{H\beta}$

However, the method that is used in this thesis do not create conventional crowning rather than a surface depended on different parameters that are analyzed thoroughly.

## 2. Design for optimal gear profiles

### 2.1 Constraints and design of undercuts

In this paragraph a code that was produced in the MD lab will be analyzed in order to have a clearer image of the profiles that are going to be created and used in this thesis.

This methodology divides in two parts. The first part is about the study of the mathematical formulation/derivation of the geometrical constraints. The second part concerns the study of various types of misalignments that develop in gears and the development of a general method of designing spur gears with misalignments while maintaining a steady transmission ratio.

### 2.1.1 Basic Law of gear theory of involution

The development of the method was based on the basic law of gear theory of the involute.

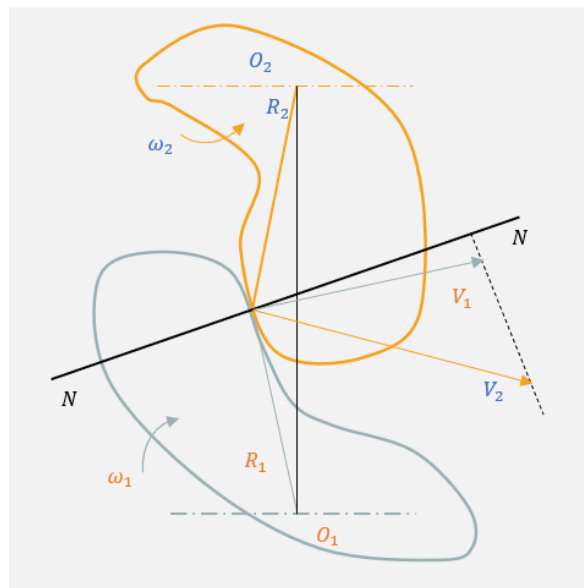


Figure 8 Condition of no penetration

$$C = (\vec{\omega}_1 \times \vec{R}_1) \cdot \vec{NN} = (\vec{\omega}_2 \times \vec{R}_2) \cdot \vec{NN} \quad (1)$$

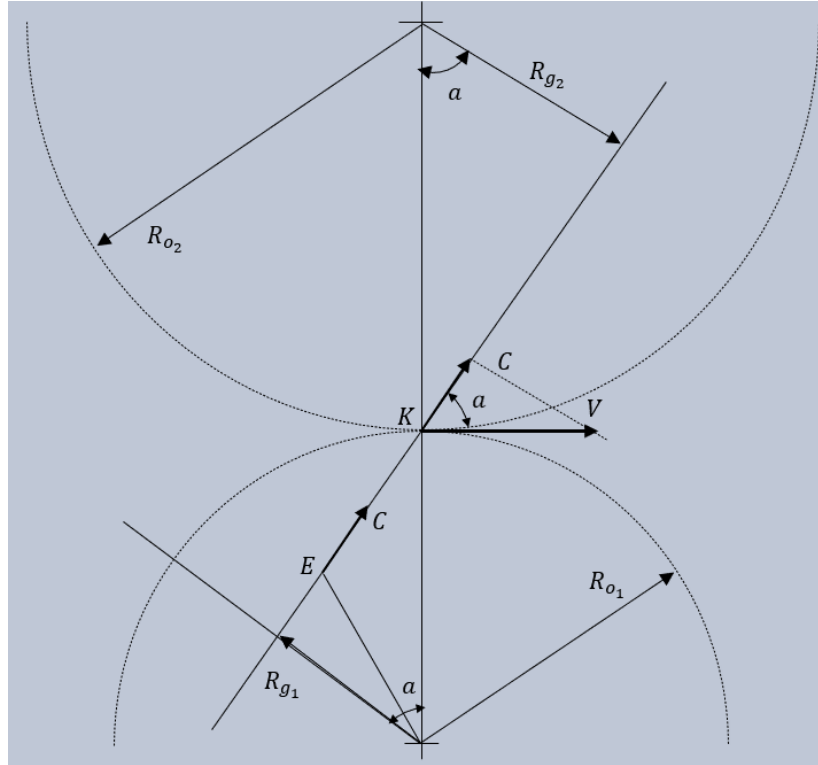


Figure 9 Condition of steady transmission ratio

$$R_{o_2} = \frac{\omega_1}{\omega_2} \cdot R_{o_1} = \sigma \tau a \theta \quad (2)$$

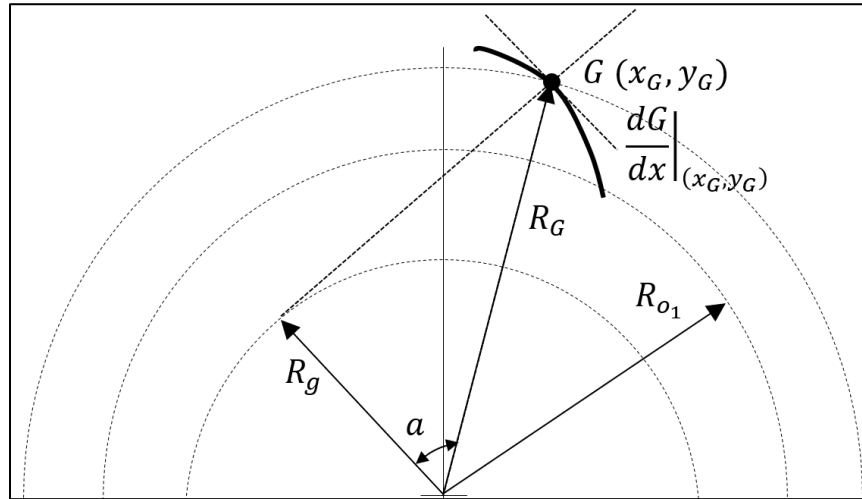
### 2.1.1.1 Theory of involution

Derived from the theory of involution the term for the basic local circle  $R_g$  was used.

$$R_g = \frac{x_G + y_G \cdot \left. \frac{dG}{dx} \right|_{(x_G, y_G)}}{\sqrt{1 + \left( \left. \frac{dG}{dx} \right|_{(x_G, y_G)} \right)^2}} \quad (3)$$

$$x_e = R_g \cdot \left[ \sqrt{\left(\frac{R_G}{R_o}\right)^2 - \left(\frac{R_g}{R_o}\right)^2} - \sqrt{1 - \left(\frac{R_g}{R_o}\right)^2} \right] \quad (4)$$

$$y_e = R_g \cdot \sqrt{\left(\frac{R_o}{R_g}\right)^2 - 1} \cdot \left[ \sqrt{\left(\frac{R_G}{R_o}\right)^2 - \left(\frac{R_g}{R_o}\right)^2} - \sqrt{1 - \left(\frac{R_g}{R_o}\right)^2} \right] \quad (5)$$



For a random point in a random profile,  $R_g$ ,  $R_G$ ,  $R_o$  define a local involute profile. From the local involute profile, the corresponding contact point is known. The theory of involution defines unequivocal and analytical, for any gear profile, the corresponding contact trajectory. However, the contact trajectory is not always on the real plane.



### 2.1.2 Geometrical Constraints during profile designing

With the theory of involution known, the method focuses on the geometrical constraints.

First, it is relatively easy to predict whether or not there could be a real contact trajectory. Intuitively, three different profile points with three different sized local basic circle and the common rolling circle are created. Thereafter, an angle  $\vartheta$  is considered to create the corresponding point as shown in figure 10. Angle  $\vartheta$  is defined by the intersection of the vertical line to the tangent line of point G with the rolling circle, more specifically point K. However, it can be observed that when the local basic circle is bigger than the rolling circle the angle  $\vartheta$  is not defined, therefore a contact point does not exist.

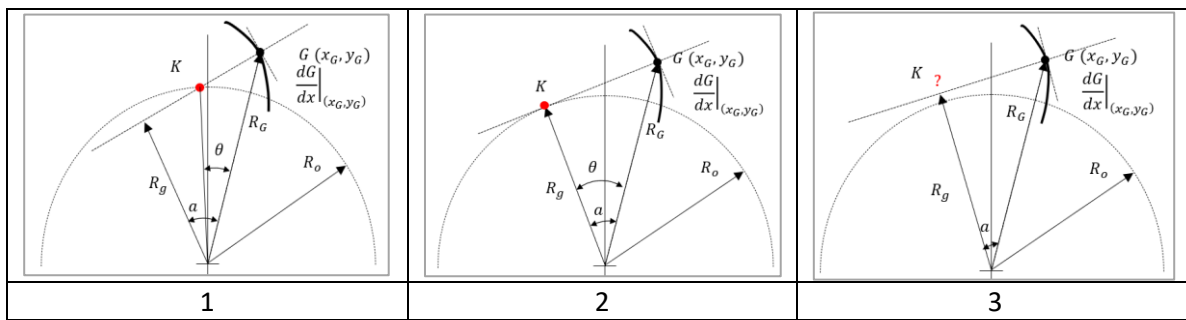


Figure 10 Different positions of point K to define angle  $\vartheta$

#### 2.1.2.1. Prediction of real contact trajectory (Geometrical Explanation)

In order to have the contact trajectory in the real cartesian plane, the involution relations need to have as input all the profile points that satisfy the requirements  $R_g < R_o$ .

- If  $R_g < R_o$  therefore the corresponding contact point is always real.
- If  $R_g > R_o$  therefore the corresponding contact point is always real
- So  $R_g > R_g$

$$\text{If } (y_G^2 > R_o^2) \quad \frac{\partial y_G}{\partial x_G} \in \left( -\infty, \frac{-x_G y_G - R_o \sqrt{x_G^2 + y_G^2 - R_o^2}}{y_G^2 - R_o^2} \right) \cup \left( \frac{-x_G y_G + R_o \sqrt{x_G^2 + y_G^2 - R_o^2}}{y_G^2 - R_o^2}, +\infty \right) \quad (6)$$

$$\text{If } (y_G^2 < R_o^2) \quad \frac{\partial y_G}{\partial x_G} = \in \left( \frac{-x_G y_G - R_o \sqrt{x_G^2 + y_G^2 - R_o^2}}{y_G^2 - R_o^2}, \frac{-x_G y_G + R_o \sqrt{x_G^2 + y_G^2 - R_o^2}}{y_G^2 - R_o^2} \right) \quad (7)$$

These relations agree with the theory of involution, because if  $R_g > R_o$  then the contact points would be on the imaginary plane.

### 2.1.2.2 Prediction of existing unacceptable edges working profile

Every gear profile is characterized either as a driver or a driven profile. The curve of the profile appears to change monotony, and this creates micro teeth that violate the no penetration criterion. In order to solve this problem, the curve of the profile was converted to polar coordinates with center the axis of the gear and it is supposed to be genuine monotonous, to avoid the micro teeth. Therefore, a parameter  $s$  was considered that runs (from 0 to 1) a random profile from beginning to end. The contact trajectory is then calculated as a function of the parameter  $s$ . Finally, it is demanded that the derivative of the function have the same sign throughout to maintain its monotony and the contact trajectory, therefore the profile of the gear.

#### Gear 1

$$G(x_{G_1}(s), y_{G_1}(s)) \quad (8)$$

#### Contact Trajectory (In cartesian coordinates)

$$y_c \left( R_{O_1}, y_{G_1}(s), x_{G_1}(s), \frac{\partial y_{G_1}}{\partial x_{G_1}}(s) \right), x_c \left( R_{O_1}, y_{G_1}(s), x_{G_1}(s), \frac{\partial y_{G_1}}{\partial x_{G_1}}(s) \right) \quad (9)$$

#### Contact Trajectory (In polar coordinates and as a center the center of the 2<sup>nd</sup> gear)

$$R_{G_c} \left( R_{O_1}, y_{G_1}(s), x_{G_1}(s), \frac{\partial y_{G_1}}{\partial x_{G_1}}(s) \right), \theta \left( R_{O_1}, y_{G_1}(s), x_{G_1}(s), \frac{\partial y_{G_1}}{\partial x_{G_1}}(s) \right) \quad (10)$$

#### Relation of the derivatives

$$\frac{\partial R_{G_c}}{\partial s} \geq 0 \Rightarrow \frac{\partial R_{G_2}}{\partial s} \geq 0 \quad (11)$$

#### 2<sup>nd</sup> Gear profile working

### *2.1.2.3 Prediction of existing double contact points*

For the final geometrical constraint there is an engineering need that needs to be covered. It is preferred not to have double contact points during the cooperation of two gear profiles, because those create dynamic phenomena. It can be observed that in order to avoid the existence of double contact point, this depends on the local curvature radius of a point compared to the norm of the corresponding line segment KG as shown in the figure 11. If the local curvature radius is bigger for every point G then it is impossible for double contact points to exist.

In order to approach the mechanism of the appearance of the double contact points as shown in the figure 11 there are some steps that need to be taken. A gear profile is considered that consists of three arches with different curvature radius comparable to the length each line segment FG.

For the blue arch with the bigger curvature radius, it can be observed that scanning through this segment from G to G' the contact point F moves counter to the rotation.

For the black arch the local curvature radius is identical with the F'G' part the point F stabilizes.

And finally for the dark blue arch with the smaller curvature radius the contact point moves with the same direction as the rotation.

As a result, the points G and G''' make contact at the same time. In order to avoid that the local curvature of the desired profile for each point is bigger than each line segment FG. In this way for a point F always exist only one point G.

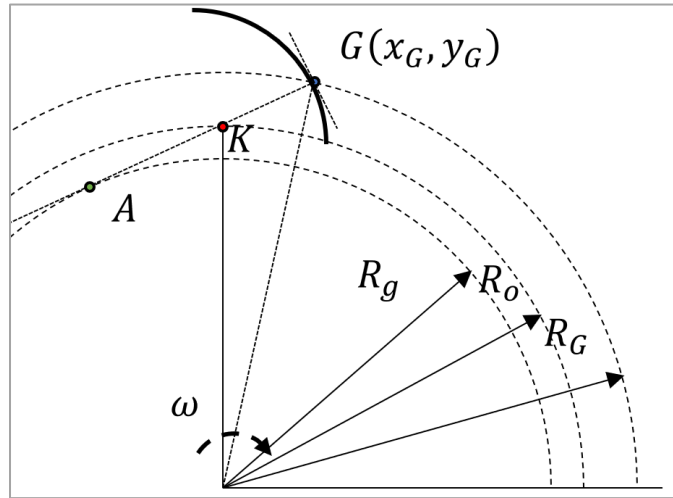


Figure 11 Curvature for point G

$$aG = \sqrt{R_G^2 - R_g^2} - \sqrt{R_o^2 - R_g^2} \quad (12)$$

$$r_G = \frac{1 + \left(\frac{\partial G}{\partial x}\right)^{\frac{3}{2}}}{\frac{\partial^2 G}{\partial x^2}} \quad (13)$$

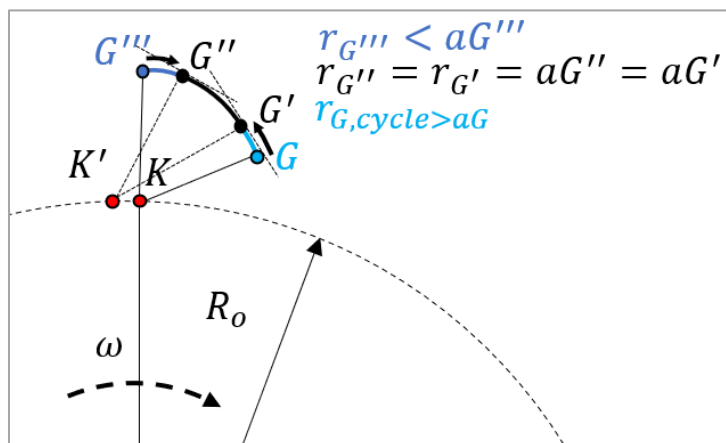


Figure 12 Avoidance of double contact points

$$\frac{1 + \left(\frac{\partial G}{\partial x}\right)^2}{\frac{\partial^2 G}{\partial x^2}} > \sqrt{R_G^2 - R_g^2} - \sqrt{R_o^2 - R_g^2} \quad (14)$$

### 2.1.3 Form Optimization with respect to Misalignments

For the second part of the designing process for the optimal profile the misalignments have to be taken under consideration

#### 2.1.3.1 Analysis of the phenomenon of the angular error

In order to approach the problem of any type of misalignment two centers of error are considered (one for each direction x and y). Also, a gear that has the misalignment is considered and a cooperating second gear that remains the same in terms of the coordinate system as shown in figure 13-14.

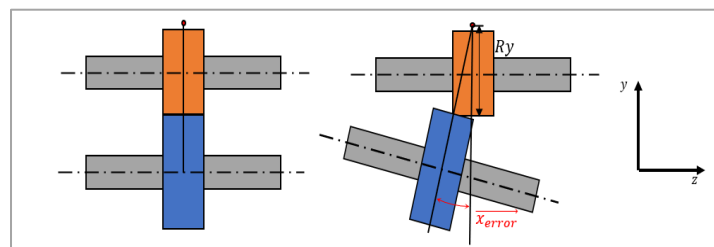


Figure 13 Error along X axis

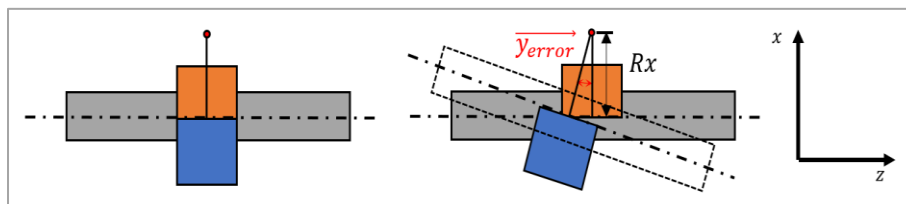


Figure 14 Error along Y axis

Eccentric gear

- Given geometry
- Takes up all the misalignment errors

## Cooperating gear

- Geometry based on the eccentric wheel and its errors

The design also takes under consideration 4 different conditions in order to be complete.

### 2.1.3.2 Analysis of the phenomenon of the angular error of 1<sup>st</sup> and 2<sup>nd</sup> different position

Firstly, two different conditions are considered for the modelling of the problem, both for the positioning of the gears.

The first position is considered according to the plane of the rolling circle (XY plane) that is due to the relative axial position of the profile with the axes of the error.

The second position is considered according to the same plane XY, but this time due to the relative position of the profile with the axes of the error in the XY direction, as shown in figure 15.

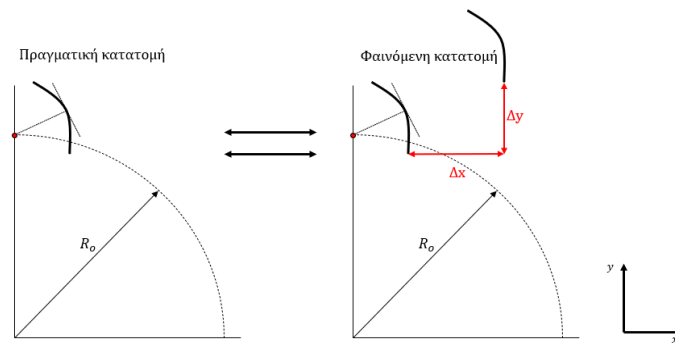


Figure 15 Differentiation due to errors

### Differentiation along the thickness from the axis of error

$$\Delta y_1 = \sin(x_{error,(rad)}) \cdot t \quad (15)$$

$$\Delta x_1 = \sin(y_{error,(rad)}) \cdot t \quad (16)$$

*Differentiation due to the distance of the contact point from the center of the errors*

$$\Delta y_2 = (1 - \cos(x_{error,(rad)})) \cdot (Ry - y_{G_{center}}) \quad (17)$$

$$\Delta x_2 = (1 - \cos(y_{error,(rad)})) \cdot (Rx - x_{G_{center}}) \quad (18)$$

As a result

$$\Delta y = \Delta y_1 + \Delta y_2 \quad (19)$$

$$\Delta x = \Delta x_1 + \Delta x_2 \quad (20)$$

*2.1.3.3 Analysis of the phenomenon of the angular error of 1<sup>st</sup> and 2<sup>nd</sup> different position and 3<sup>rd</sup> along the thickness direction*

As a third condition, a different position is considered along the axial direction, due to the relative position of the profile to the axes of error along the XY directions.

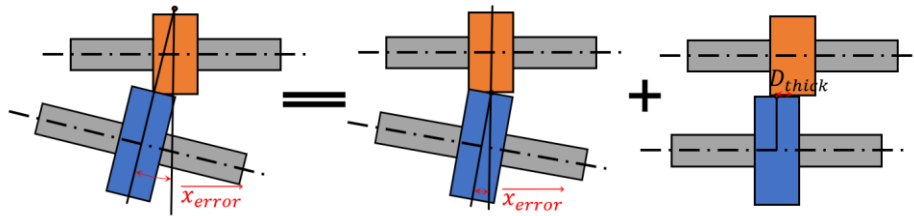


Figure 16 Overlapping X and Z error

$$D_{thickness} = (Ry - y_{G_{center}}) \cdot \sin(x_{error}) + (Rx - x_{G_{center}}) \cdot \sin(y_{error})$$

*2.1.3.4 Analysis of the phenomenon of the angular error and 4<sup>th</sup> different vertical contact velocity*

The fourth and final condition is the differentiation of the velocity vertical to the tangent line of the contact points due to angular errors.

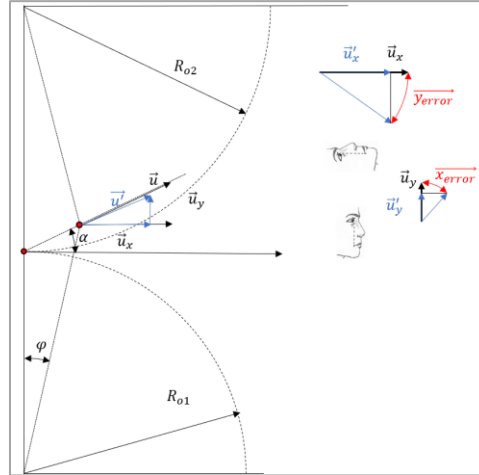


Figure 17 Differentiation of speed

$$u' = u \cdot \sqrt{(\cos(\varphi) \cdot \cos(y_{error}))^2 + (\sin(\varphi) \cdot \cos(x_{error}))^2} \quad (21)$$

#### 2.1.3.5 General Design Method based on the 4 different conditions

From the profile that has taken the misalignment error the design of the profile is proceeded with the new corrected working profile.

More specifically there are some steps that need to be followed in order to complete the method.

1. The angle  $\theta_1$  of  $G_{1,before}$  is calculate and then the profile is rotated along the angle  $\theta_1$
2. The displacements  $\Delta_x$  and  $\Delta_y$  are applied along the whole profile
3. Taking under consideration  $G_{1,trans}$  the ratio of the apparent speed  $\frac{u'}{u}$  is calculated.
4. In the newly displaced profile  $G_{2,trans}$  a new contact point is required.
5. After acquiring the corresponding contact point the  $G_{2,trans}$  is rotated with angular velocity
 
$$\omega_2 = -(\omega_1 \cdot \frac{u'}{u}) \cdot \frac{R_{o1}}{R_{o2}}.$$



6. Finally, the point  $G_{2,after}$  has returned to its original position  $G_{2,before}$ .
7.  $G_{2,before}$  is granted the property of thickness based on the relation  $Thickness_{Gear1} + D_{thickness}$  and is calculated.
8. This procedure is repeated for every point of the profile of the eccentric wheel

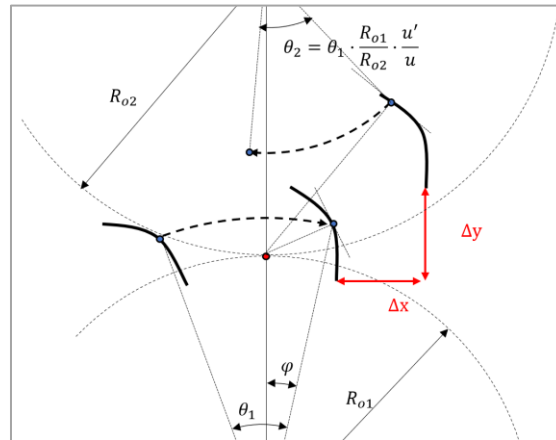


Figure 18 Final theoretical Result

After completing the procedure, it is of the utmost importance that the results are verified.

## 2.2 CAD of the Modified Profiles

In this paragraph KISSOFT, SOLIDWORKS to verify the results and produce the final profile of the gear before the FEM analysis.

### 2.2.1 Design Trials

In order to confirm the results of the aforementioned methodology they should be tested in CAD to see if the results agree with the thought and the execution of the MATLAB program.

### 2.2.1.1. 1<sup>st</sup> Test

To create the computed profiles a set of data is generated by the MATLAB code. The code requires as inputs the module, the number of teeth and the misalignment error that exist in order to generate said data set.

The cloud point that is generated is then inserted into SOLIDWORKS as curves.

To assure the profiles would show results the positions of the surfaces were made to be tangent. Thereafter, a theoretical transmission ratio was applied and during the rotation it could be observed that there were no gaps or penetration of one geometry to another.

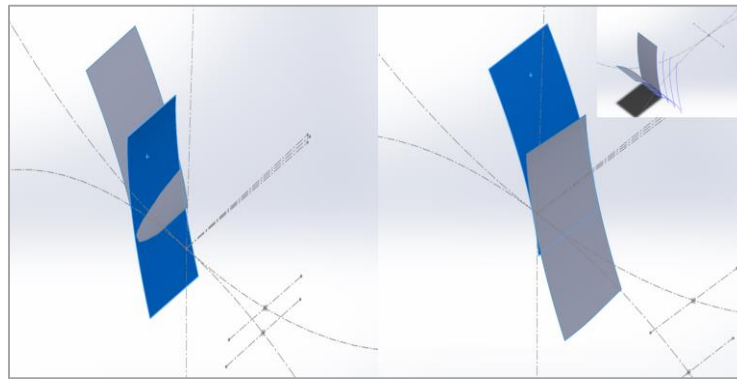
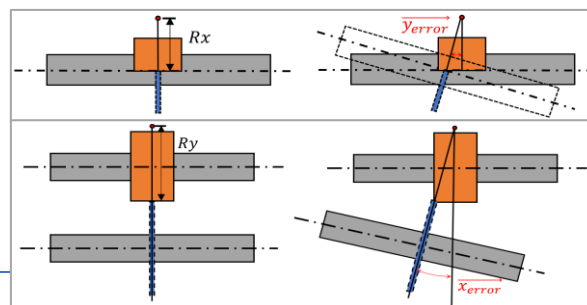


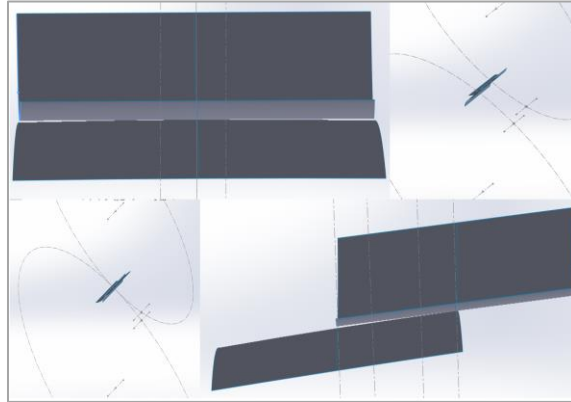
Figure 19 1st Test

### 2.2.1.2 2<sup>nd</sup> Test

After the 1<sup>st</sup> test the profiles should be tested in different angular errors.

In this test the design was done using the 1<sup>st</sup> profile of the computed data sets, because it is the one that penetrates the furthest while applying different errors. In this case, the cooperation was good for the different applied misalignments.

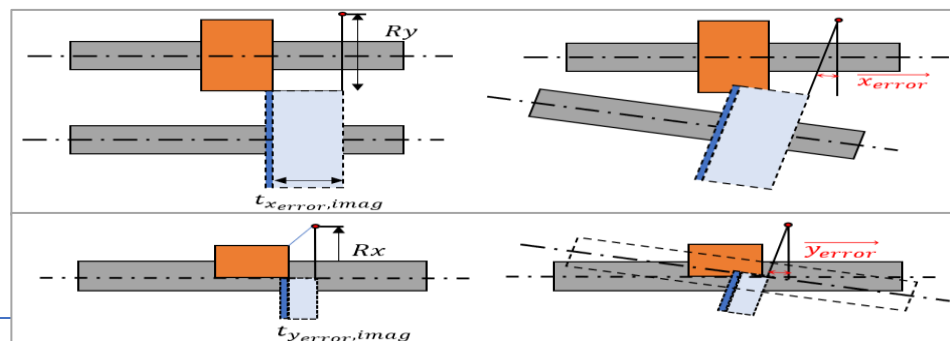
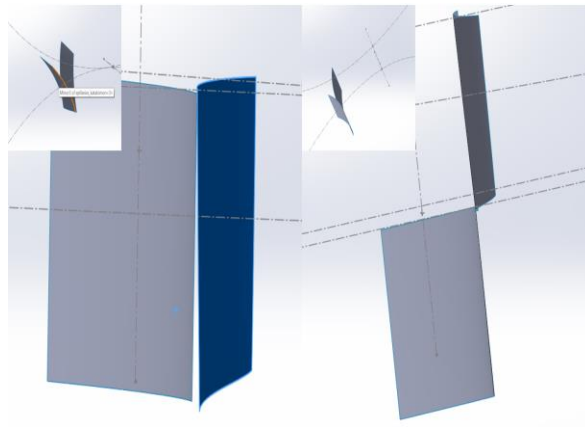




### 2.2.1.3 3<sup>rd</sup> Test

For the final test the center of the error was considered in a different axial position. The profiles were designed using different angles and the furthest from the center produced profile, because it was the one that penetrates the furthest.

The cooperation of the profiles was as good as the previous ones.



### 2.2.2 Gear assemblies using KISSSOFT and SOLIDWORKS

In this chapter the procedure that was followed to create working gears is going to be decomposed. In order to have a way of producing gears with the optimal profiles with the previous method a way for consistently producing gears was needed.

#### 2.2.2.1 KISSSOFT Gears

After the computation of the optimal profile gears with MATLAB in module 1.5 and 0.4 it was necessary for the study to have the whole gear. Therefore, knowing the parameters number of teeth and distance from the center of the gears, KISSSOFT was used to extract the 3D MODELS as shown in figure 20.

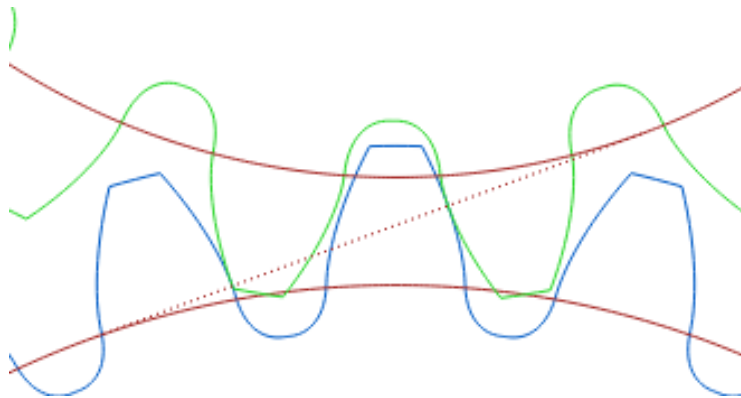


Figure 20 Involute profile  $m=1.5$

The KISSSOFT models were then inserted into SOLIDWORKS to perform the necessary changes in order to have the optimal profiles that were computed.

KISSSOFT gears both the driver and the driven have the involute profile generate by the program. However, in this thesis the gears have modified profile in order to accomplish there were some steps that need to be followed.

#### 2.2.2.2 SOLIDWORKS Designing

The geometries produced by KISSOFT were inserted in SOLIWORKS and two separate assemblies needed to be created to have a clearer image of the problem.

The first assembly had the gears produced by unchanged as a control. The second assembly has the gears as the first on with the same center distances and all. However, the key difference is that in this assembly the data set computed by the MATLAB code is inserted. The first data sets contain the unchanged involute profile of the gear that is going to be used as control. The second data sets contain the modified profile.

#### 2.2.2.2.1 Control Gear Assembly

In order to check the results of the MATLAB code the profile of one of the KISSOFT produced gears is mated with the generated profiles. If the involute profiles did not mate, then the code would not produce correct profiles as it was planned to do. However, the profiles produce by the code mated with tangent relation with the KISSOFT produced gears. That meant that the code was working properly, and the modelling could continue.

In this thesis, the second gear which would have the modified profile is the conjugate gear, because it is going to be used further in the planetary gear train as the sun. Therefore, after inserting the second data sets with the rolling circles and the center of the gear produced by MATLAB code the conjugate gear produced by KISSOFT was inserted.

It was mated to be concentric with the center of the theoretical gear by MATLAB. Then using the first set of the second data sets it was calibrated to be tangent with those data. Those data always produce the central plane of the gear and it contains the profile that is involute. Therefore, it can be used as in the first gear as a control to see if the code is working properly and to have a point of reference for the rest of the profiles as shown in figure 21.

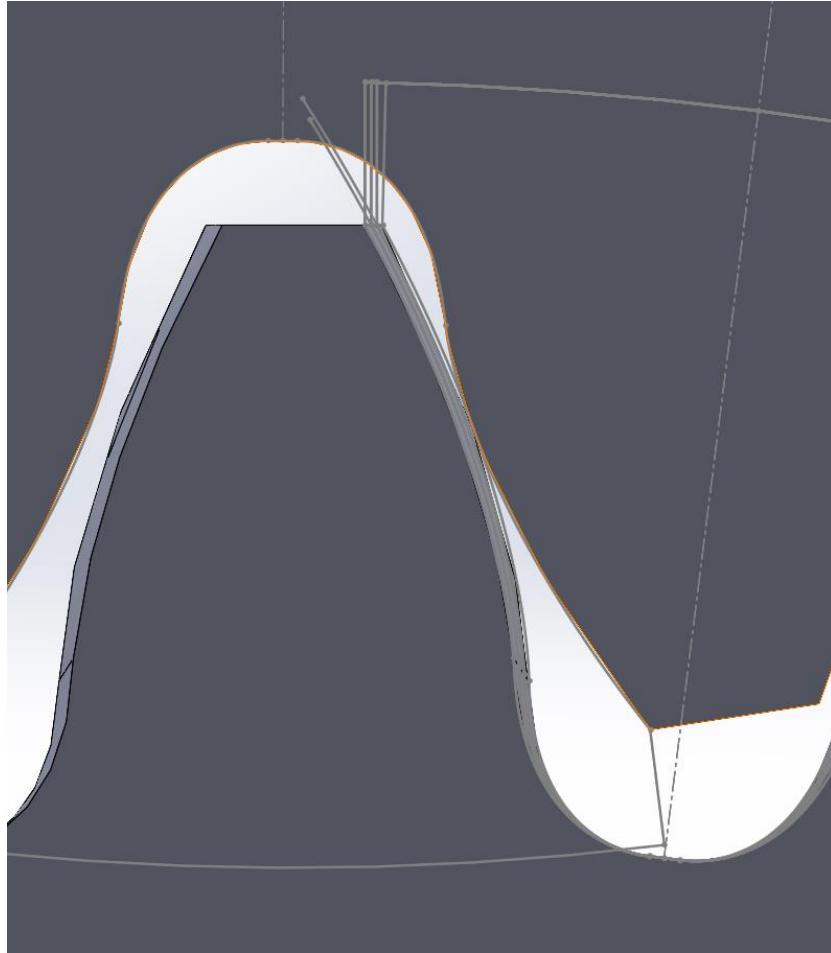


Figure 21 Tangent Involute Profiles

The initial conditions of the MATLAB as was written above was the module, the number of teeth and the misalignment error. However, there is an extra condition that provides better quality of the produced modified involute profile. The number of planes determine the precision of the profile along the facewidth of the tooth. The number of planes required for the certain model in order to be precise enough and not redundant was 4 planes. One central plane and three more along the facewidth.

#### 2.2.2.2.2 Modified Gear Assembly

To create the modified profile in the assembly the conjugate gear was edited as part in order to convert the segments of the profile from the different planes to the corresponding planes in the part.

After converting the desired entities to each corresponding plane, the editing of the part in the assembly is finished. The next part of the process requires only the conjugate gear, so the assembly is closed and the part alone is opened. In the part it can be seen that the converted entities from the assembly have been transferred to each of the planes as it was desired. Then, using the Loft cut command and connecting the profiles the modified profile is created as shown in Figure 22.

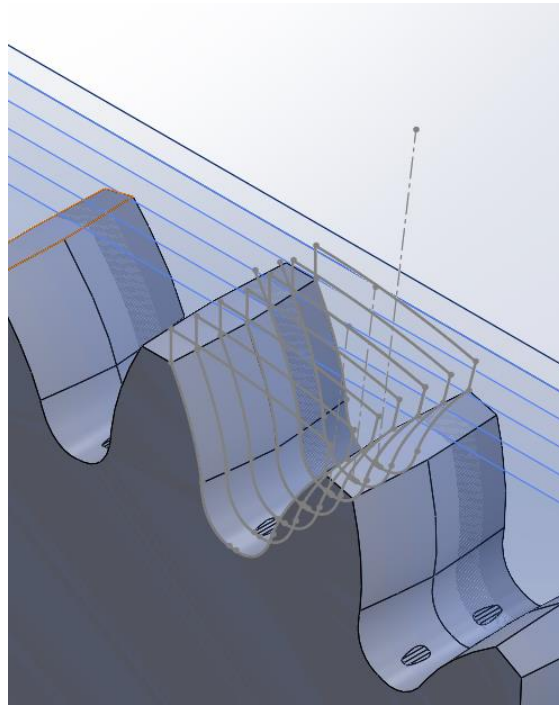


Figure 22 Scanning of the tooth facewidth

### 2.2.2.3 Finished Gear Assemblies

The final product then can be seen in the SOLIDWORKS assembly. The gears mesh correctly and using the identify penetration tool it can be tested where the gears make contact. As expected, the control assembly of gears from KISSOFT with parallel planes make contact along the whole facewidth of the tooth. The gears in the assembly with the modified profile make contact in a certain point with parallel planes. If the gears are not parallel but misaligned the control assembly have penetration in certain area at the edge of the tooth. The modified assembly again has contact only at a certain point of the profile further confirming the workability of the code and its ability to have a better transmission and minimum deformation.

However, because SOLIDWORKS is not accurate enough ANSYS will be used in order to ascertain whether the modified profile has less deformation and stresses in a misaligned plane than the control involute group.

## 3. Overview of the mechanical phenomena

In this chapter the mechanical phenomena that are going to be encounter are explained thoroughly. There are certain phenomena that this thesis tackles, as it has been mentioned the model that is studied is a plastic PGT with misaligned spur gears due to forces acted upon the rollers attached to the gears from the tube. Those phenomena can be broken down to separate problems to be more understandable. The phenomena that are going to be studied are the contact of the plastic gear in static stress analysis, misaligned contact of gears, the effect of the misalignment in a PGT in a transient analysis and the compression of a silicon-based tube with variable fittings of the rollers.

### 3.1 Contact Theory with and without Misalignments in one-stage pair of gears

The contact of metallic gears has been thoroughly studied in the bibliography and it is a very important phenomenon with great implications in the industry. However, in this thesis the material of interest is plastic and based upon studies done for the plastic gear it is going to study the contact stresses and deformation in a static analysis in ANSYS.



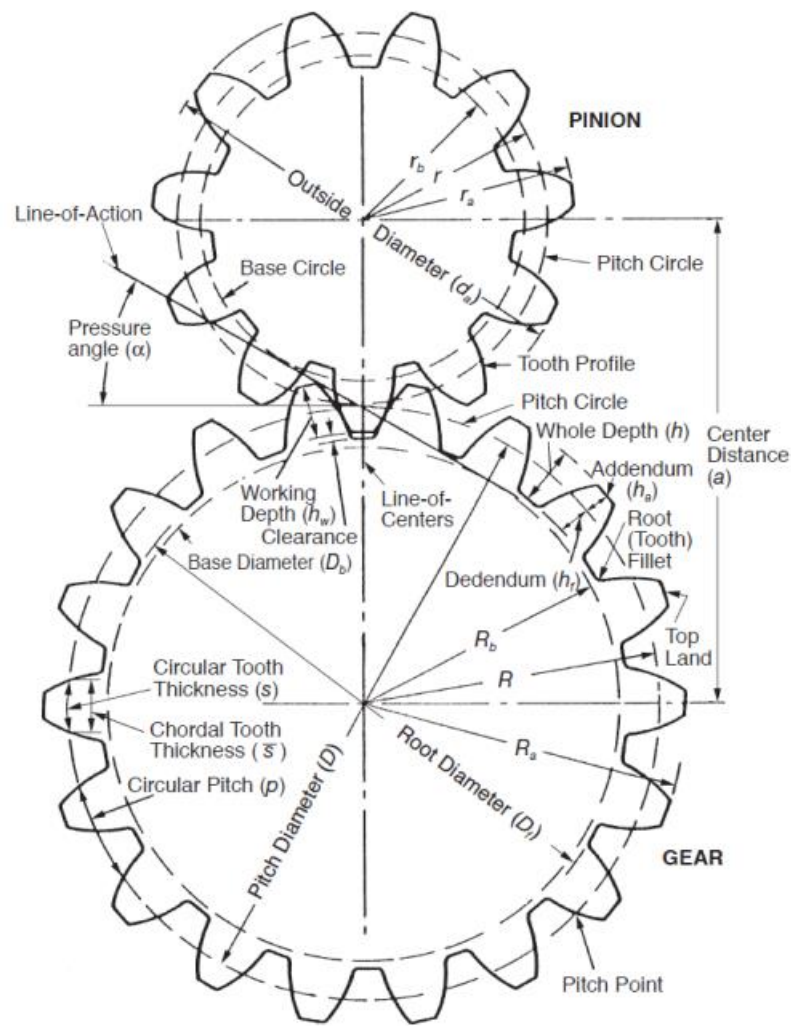


Figure 23 Basic Gear geometry

The contact stresses occurring during meshing of two gear teeth can be estimated using Hertzian theory. This well-established theory is used in most of the standardized calculations. The contact stresses can be expressed as function of the load, contact stiffness, reduced radius of the contact and the width of the contact, according to:

$$\sigma_{Hz} = \sqrt{\frac{FE_r}{2\pi bR_r}} \quad (32)$$

Where  $F$  is the force (load),  $E_r$  reduced modulus or contact stiffness (see equation 33),  $b$  is the width of the gear and  $R_r$  is the reduced radius of the contact (see equation 34).

$$E_r = \frac{1}{2 \left( \frac{1 - \nu^2}{E_g} - \frac{1 - \nu^2}{E_p} \right)} \quad (33)$$

Where  $E_r$  is the Young's modulus and  $\nu$  is the Poisson's ratio of the gear.

$$R_r = \frac{1}{\left( \frac{1}{R_g} - \frac{1}{R_p} \right)} \quad (34)$$

where  $R_r$  is the local radius of curvature of the tooth flank of gear/pinion.

Misalignments are a very common occurring phenomenon with gears, either due to manufacturing errors on the axes or the gears themselves or even in the assembly. Therefore, it is critical to have a better understanding and modelling of the phenomenon in order to deal with it. Misalignments have been known to cause vibrations and contact nonlinearities, which in turn cause load distribution shift on the gear tooth. [3] The load distribution shift of the gear pair results in increased contact and bending stresses with the maximum stresses leaning towards the edge of the face width. These stress changes cause failures and gear performance variations, such as pitting, scuffing, crack initiation and eventually tooth breakage. In this paper, the contact and bending stresses of a misaligned spur gear pair were evaluated by employing corresponding analytical methods and finite element method (FEM). The stress concentration was found to be higher at the contact point and at the tooth root of the gear with the augmentation of the misalignment distance and angle. Finally, the relationships between the normalized stress and misalignments (both axial and angular) were established.

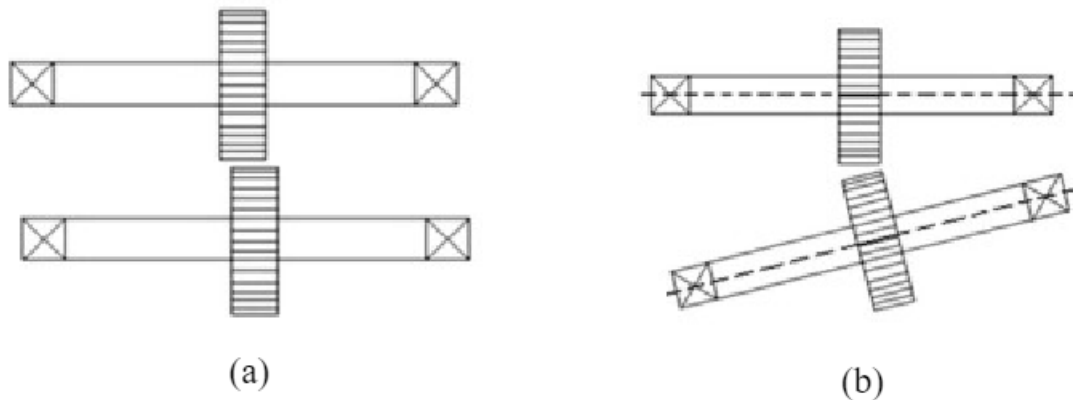


Figure 24 Gear Misalignment (a) axial (b) angular

Misalignments in gears are considered as one of the major contributing factors for increased stress concentrations at specific locations of the gear tooth. The stress concentration region is the initiation point of a failure or fracture of the gear tooth. Recent research has concentrated on using the FE approach to determine the stress concentrations on the spur gear tooth.

Frictional stress analysis of spur gear with misalignments concentrations generated due to misalignments influence the gear tooth contact stresses significantly. Hence the study of the effects of misalignments on gear contact stresses is important. In gear contact, the gear misalignments imply the axial shift in position of the mating surfaces due to deflections or errors in manufacturing of the gear and their housing. The main causes of misalignments on the gear are lead slope errors, lead wobble, bore parallelism and shaft bending deflections. Several studies and research have been conducted and different methods have been used for the stress analysis on the misaligned gear teeth.

There are three types of misalignments in a gear shaft which are parallel misalignments, angular misalignments parallel to the plane of action and angular misalignment perpendicular to the plane of action.

The studies conducted on the stress distribution of gear subjected to the axial misalignment condition. They found that the equivalent stresses at the root increased almost twice as the equivalent stresses at the contact region. The stress concentration was found to have increased proportionally to the misalignment angle at the contact region and at the tooth root. Bending stress analysis is also an important objective of static performance investigation because it is the primary reason of various gear tooth failures. Bending stress is investigated in similar fashion to that of a contact stress investigation. The only difference between the two is that the bending stress depends on the gear tooth geometry compared to contact pressure which is much straight forward evaluated the bending stress on the spur gear tooth with angular

misalignments and discovered that the bending stress and load distribution factor increases with the increasing misalignment angle. The load is assumed to be uniform when the gear contact is aligned as shown in Figure 25(a) but when misalignment occurs the load will be shifted to the gear tooth flank as shown in Figure 25(b).

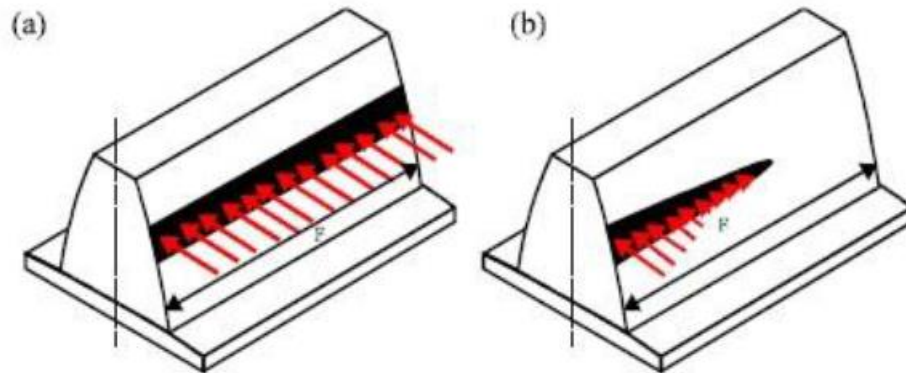


Figure 25 The load distribution of gear surface (a) aligned (b) misaligned

### 3.2 Contact Theory of a PGT

Torque is transferred from one gear to the other through tooth contact. Depending on the tooth geometry, various amounts of sliding can occur. Sliding results in wear and it is therefore important to minimize the amount of sliding that occurs in the contact. One important feature in minimizing sliding is the curvature of the tooth, which usually follows an involute function. An involute profile ensures that the force vector or line of action (figure 26) is perpendicular to the surface at every point along the contact path. Figure 26 shows how the involute profile is generated, depending on the size of the tooth.

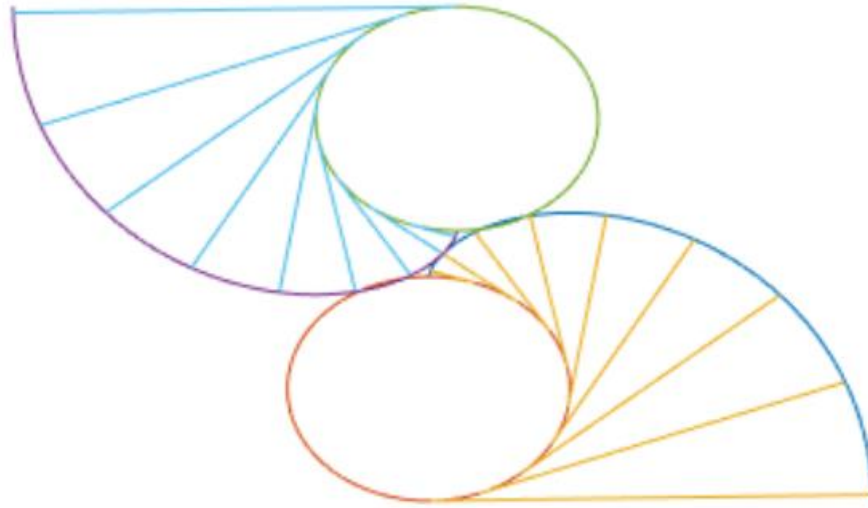


Figure 26 Involute profile and tooth-to-tooth contact

Due to manufacturing and elasticity, there will always be some misalignment of the involute profiles and deformation of the tooth surface, leading to wear and fatigue. Misalignment between the contacting teeth occurs due to twisting and bending of the internal components of the gearbox, such as shafts, carriers, and the housing. The misalignment leads to non-symmetric stress distribution across the face of the gear tooth and stress concentrations which can be explained by studying the spline connection.

Following the ISO 6336-2 (2006) standard, nominal contact stress values are given by formula (12):  $\sigma_{H0} = Z_H Z_E Z_\epsilon \sqrt{F' d b \cdot u + 1} u$  (35)

where:  $Z_H$  – zone factor,  $Z_E$  – elasticity factor,  $Z_\epsilon$  – contact ratio factor,  $F'$  – circumferential force,  $d$  – drive gear pitch diameter,  $b$  – ring width,  $u$  – gear pair ratio. [4].

### 3.3 Kinematic analysis of PGT and the system and simplification of the model

#### 3.3.1 Decoupling of the system

For the transient analysis of the system, it was critical that the model run as a whole to demonstrate as realistic as possible the phenomena that develop during the operation of the pump. However, due to computational limitations as well as unexpected phenomena due to the nature of the model, it was decided that the decoupling of the system was necessary.

The decoupled system consists of two different mechanisms. The PGT and the roller-pump-carrier system (RPC). In order to achieve the decoupling, it was necessary to consider how each system influenced the other.

The PGT is the power train of the whole mechanism that moves the roller pump, therefore this motion should be included in the RPC system, so that the rotational motion is captured in the rollers as well as the tube.

The RPC on the other hand produces frictional forces, moments and misalignments on the PGT that will be later added in FEM analysis to simulate as close as possible the effects of the pump on the PGT.

Therefore, the decoupling of the model simplifies the problem as a whole and reduces computational power but also reduces the accuracy of the model. However, with certain constraints it will assure a certain accuracy that is going to be exploited to evaluate the results.

### 3.3.2 Kinematic analysis of a PGT

The kinematics of a PGT are known in the bibliography and are worth mentioning in this study.

Planetary gears have a wide range of use as they provide a compact design, capable of transmitting high torques and achieving high gearing ratios. A planetary gear system consists of a sun gear, a set of planets and a ring gear. The layout of a typical system is shown in figure 27. The figure shows the most common configuration where the sun acts as the input and the planet carrier acts as the output, resulting in the highest gearing ratio [5]

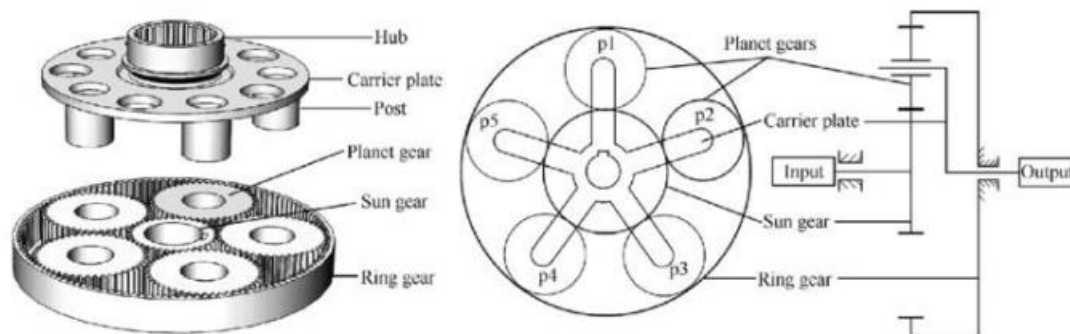


Figure 27 Structure and schematic diagram of a planetary gear train

The gearing ratio for a planetary gear system depends on the configuration of the system as well as the individual gears. Figure 28 illustrates the motion of the planets which is described by equations 36-42.

Considering the planets rotation around the sun due to the carrier's rotation:

$$\phi_{p1} = \phi_c \quad (36)$$

The planets rotation around its own axis due to the carrier's rotation:

$$\phi_{p2} = \phi_c r_s r_p \quad (37)$$

Where  $r_p$  and  $r_s$  is the radius of the planet and the sun. And the planets rotation around its own axis due to the sun's rotation:

$$\phi_{p3} = -\phi_s r_s r_p \quad (38)$$

Gives through super positioning of the individual motions:

$$\phi_p = \phi_c + \phi_c r_s r_p - \phi_s r_s r_p \quad (39)$$

Which can be written as:

$$n_p r_p = n_c (r_p + r_s) - n_s r_s \quad (40)$$

Where  $n_p$ ,  $n_c$  and  $n_s$  is the revolution of the planet, the carrier, and the sun. Given that  $\phi = 2\pi n t$ , where  $t$  indicates time [6]. Or with the number of teeth as:

$$n_p z_p = n_c (z_p + z_s) - n_s z_s \quad (41)$$

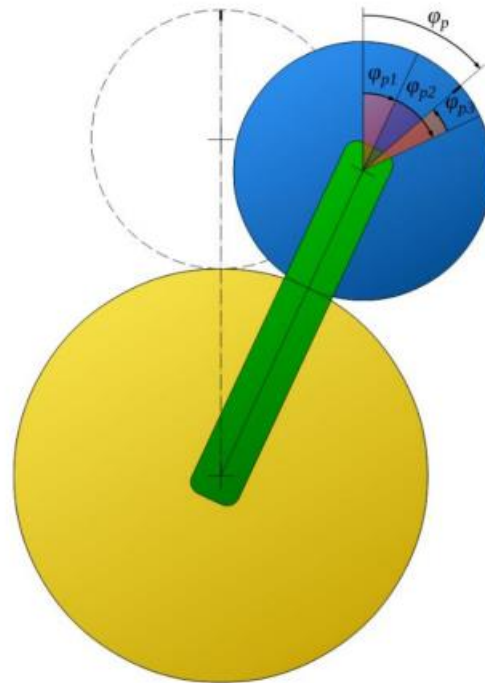


Figure 28 Superposition of motions

The relationship between the velocities  $V_r$ ,  $V_p$ ,  $V_c$  and  $V_s$  of the gear is described in figure 29 and is determined by equations 42-43.

$$V_r = V_p + V_c \quad (42)$$

$$V_s = V_c - V_p \quad (43)$$

Which eventually gives the velocity of the planets as:

$$n_{prp} = (n_{rrr} - n_{srs})/2 \quad (44)$$

Given the peripheral velocity  $v = 2\pi n$



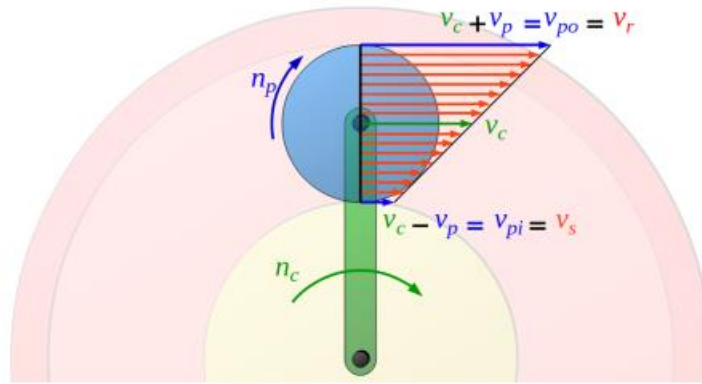


Figure 29 Velocity distribution on the rotating planet gear with moving carrier

Combining equation 2.5 and 2.9 gives:

$$n_r r_r = n_c (r_r + r_s) - n_s r_s \quad (2.10)$$

Or

$$n_r z_r = n_c (z_r + z_s) - n_s z_s \quad (2.11)$$

For the configuration where the ring gear is fixed, equation 2.11 gives the gearing ratio as:

$$n_s n_c = i = z_r + z_s z_s = 1 + z_r z$$

### 3.3.3 Modelling of the system in SOLIDWORKS

Before the initial testing of the RPC and the PGT system it was deemed necessary to run the whole model through a rigid body dynamic analysis. This was done using motion analysis in SOLIDWORKS which enables the analysis of the model without great computational power.

The model of the pump was inserted in the motion analysis. The boundary conditions of the model determined the contact of its body. Therefore, the gears had contacts with each other, the carrier and the tube. However, the tube was replaced by a thin sheet of metal that simulated the tube via the use of springs, as it was computationally more strenuous as shown in figure 30.

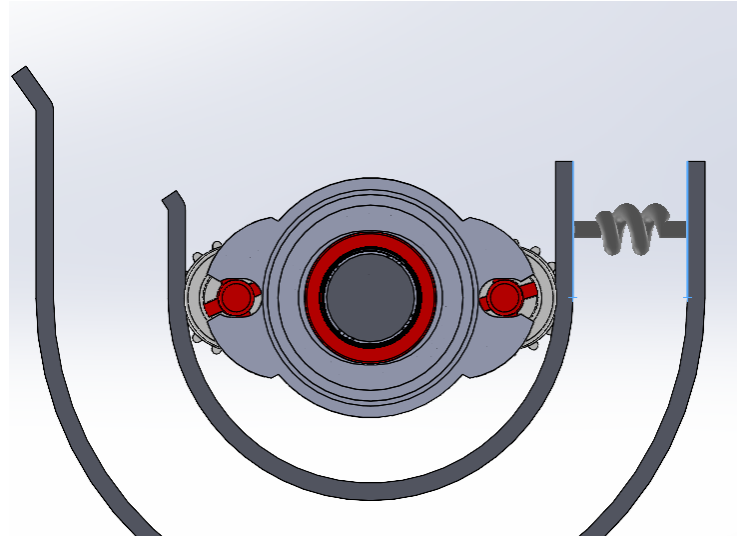


*Figure 30 Model of the pump in Motion analysis*

A shaft was then added to the model in order to simulate the shaft of the motor that was going to rotate the sun and the whole system. The motor was set to rotate at 10 RPM to match the actual rotation of the pump. After setting the boundary and the initial condition the model run.

The trajectories of both the planets and the sun were calculated by SOLIDOWORS. They show a relatively mild vibration but that is due to the fact that the model is rotating at such a low speed and the ring has as a very tight support that does not allow the sun to wobble. Also, the trajectory of the planets follows the predicted pattern of a point on a planetary system and do not wobble as well. That is also because the model has very low speed and tight boundary conditions.

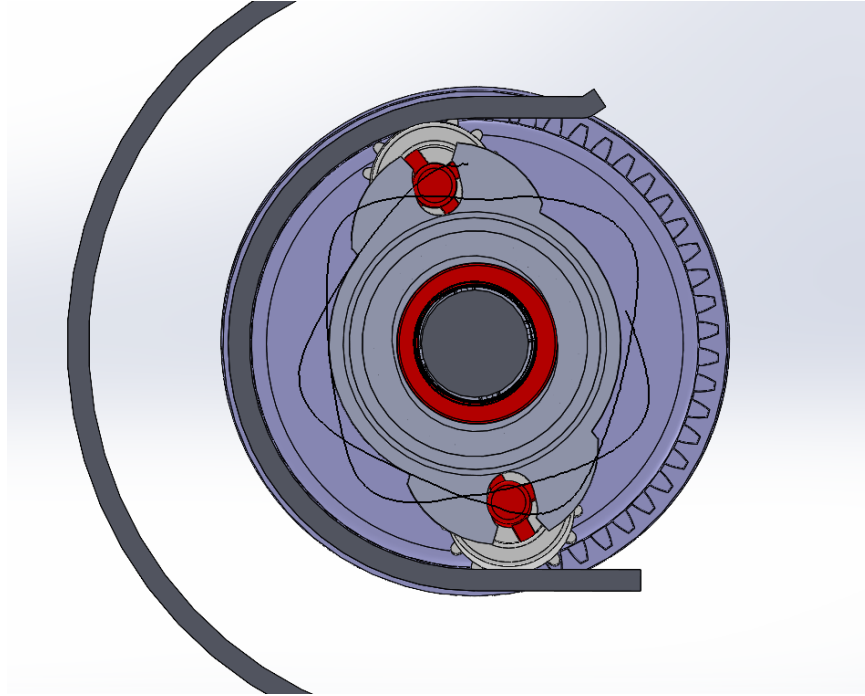


Figure 31 Trajectories of the planets and the sun

This whole model gives a very good insight in the workings of the pump and what must be done to model it in ANSYS Workbench.

## 4. FEM Analysis in Ansys Workbench

In this chapter the CAD models that were produced and designed either with KISSSOFT or by the MATLAB code are going to be tested either in static or transient analysis in order to ascertain their behavior under certain conditions and compare them with each other in the following chapters.

### 4.1. Three-dimensional modelling of involute spur gears

#### 4.1.1 Static Analysis of the cylindrical gear pair and the PGT

First and foremost, the static analysis of plastic gears is of utmost importance, because from its conclusions are going to be extracted vis a vis the deformation, the von Mises stresses and the contact pressure of the gears, either in pair or in the PGT. The gears are going to be submitted in these tests either as planar problems or as misaligned, both of which need a certain method in order to be set correctly. In the following paragraphs the static models of the three-dimensional spur gears in pairs and in the PGT are going to be fully analyzed.

##### *4.1.1.1 Modelling of involute spur gears*

The CAD models of the gears were created in KISSOFT and after completing the design process in SOLIDWORKS were imported into Design Modeler of Static Structural of ANSYS Workbench.

The assembly of the gears was initially done using SOLIDWORKS, however SOLIDWORKS is not an accurate enough tool to position them correctly. Therefore, the positioning was done using Design Modeler of ANSYS to avoid unwanted penetrations and/or gaps. To insert the model in ANSYS workbench, when workbench is opened right click on the white background area. There a window will appear with several choices. At import the geometry of the study will be imported. In order to import any file in ANSYS it should either be in STEP format, or STL format or usually in IGES format. So, after inserting them into Design Modeler, there angles were computed using MATLAB.

With known angles the models were then modified in DM. In order to achieve the desired angle for the gear contact in DM the Rotate tool was used which is found in Create → Body transformation → Rotate and the rotation of the object depends on the plane selection in axis definition and the sign of the angles on the direction of the axes of rotation. After having defined the angles to reduce computational power and the gears were sliced as shown in figure 32, because the regions of interest in the static analysis are only the ones that come in contact, therefore the gear teeth.

Lastly, two cylindrical bodies are created at the points of contact as shown in figure 32

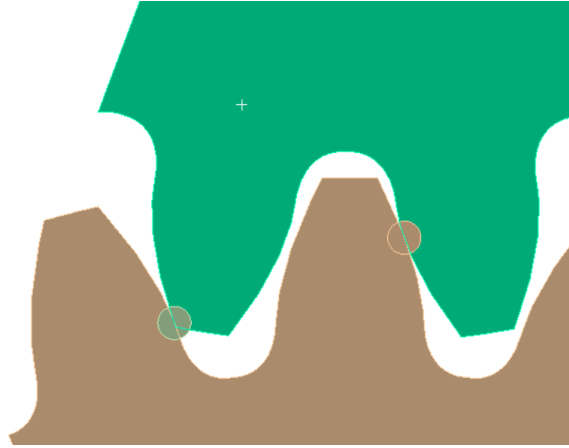


Figure 32 Cylindrical Bodies in DM

These bodies will be used later in the meshing process. However, it is preferred that they are created in the DM before starting the Static structural analysis to save both time and limit the possible mistakes especially in the Connections/Contacts section afterwards.

#### 4.1.1.1.1 Static Analysis

After finishing the model in DM in the Workbench environment there should be a choice where it says static structural by clicking on it and then inserting the geometry in the study the analysis can begin.

#### 4.1.1.1.1.1 Material

The material used for this model was plastic and more specifically PVC (Polyvinyl Chloride) The selection of this material is explained in the previous chapters. Therefore, after the material choice it must be inserted in the ANSYS model. In order to do that, the section Engineering data must be selected. There by selecting Engineering Data Sources the materials offered by ANSYS are found. Then the desired material is chosen. However, in this case the material is different than the default ones, therefore it is made. To create the material ANSYS have options for the properties of the material.

## 4.1.1.1.1.2 Contact parameters

The most important part of this study is the way the gears make contact. By default, when opening the model in ANSYS at the contact selection it may already contain possible contacts that the program has predicted. However, those are not desired, therefore they should be deleted. Then by right clicking at Contacts from Connections → Contacts → Insert it shows to insert a manual contact region. Choosing that the following parameters should be changed as shown in figure 33.

☐ Scope	
Scoping Method	Geometry Selection
Contact	1 Face
Target	1 Face
Contact Bodies	Solid
Target Bodies	Solid
Protected	No
☐ Definition	
Type	Frictional
<input type="checkbox"/> Friction Coefficient	0,2
Scope Mode	Manual
Behavior	Auto Asymmetric
Trim Contact	Program Controlled
Suppressed	No
☐ Advanced	
Formulation	Augmented Lagrange
Small Sliding	Program Controlled
Detection Method	On Gauss Point
Penetration Tolerance	Program Controlled
Elastic Slip Tolerance	Program Controlled
Normal Stiffness	Factor
Normal Stiffness Factor	10,
Update Stiffness	Program Controlled

Figure 33 Contact Parameters

This must be done for both contact regions of the gear teeth with the same parameters as shown in figure 34.

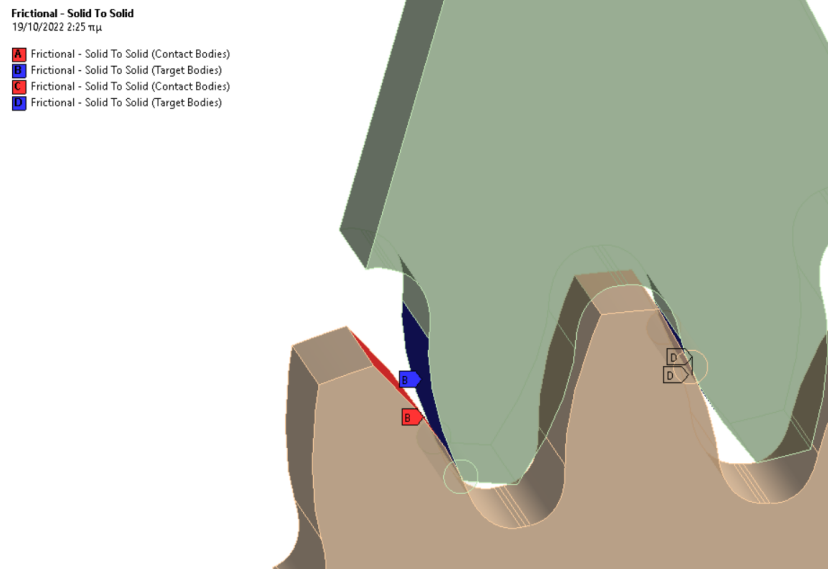


Figure 34 Final contact regions

In order to assure that the contacts that have been made are correct by right clicking on Contacts→ Contact Tool is created and then by right clicking the newly made contact tool→ Insert general information. The general information panel will show whether the gears show any gaps or penetrations. The optimal initial information for this kind of study.

#### 4.1.1.1.1.3 Meshing

Correct meshing is essential in any study as it can affect both the computational power needed and the results. The easiest and less user demanding way of meshing a structure is to use tetrahedral elements, these elements are highly adaptive and can be automatically applied to any geometry. An alternative to tetrahedral elements could be to instead use hexahedral elements. Hexahedral elements are generally considered to be better than tetrahedral since they can be used more efficiently to mesh parts that are of low interest. The reason for this is that HEX elements can have large aspect ratios, meaning that the elements can be made long and fill a larger volume of the geometry. TET-elements, however, require an aspect ratio that is close to one, meaning that all sides of the TET-element must be near equal. This means that many elements must be used to cover the same volume as one HEX-element. Most FE-software achieve convergence by continuously reducing the element size, this approach is known as the H-method, the alternative is known as the P-method, and means that instead of reducing the element size, the element order is increased. Increasing the element order increases the number of nodes, a 1D linear element consists of two nodes, and a quadratic element consists of three nodes and so on. Software that achieves convergence through the H-method often only provides linear or quadratic elements. The option to use quadratic elements is often useful

since linear elements can experience shear locking. Shear locking occurs when a geometry meshed with linear elements is subjected to bending. A deformed linear element can be seen in figure 35. The figure shows that the bending moment, (represented by a tensile and compressive force) causes the horizontal sides to compress and elongate, this causes the vertical sides to twist from their 90 degree angle, indicating that the element contains shear strains, which should not exist in pure bending.

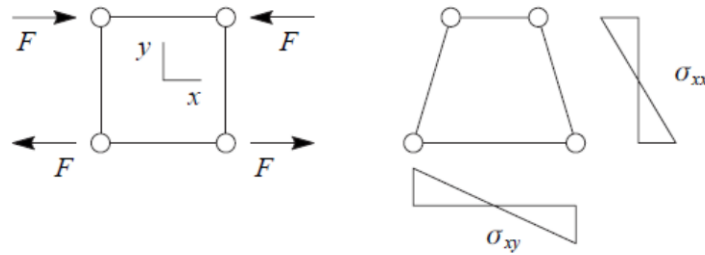


Figure 35 Deformation of a linear element under pure bending

Figure 36 shows the deformation of a quadratic element. Due to the quadratic elements ability to represent a curved surface, it is possible to maintain the 90-degree corner between the horizontal and vertical sides and prevent shear strains.

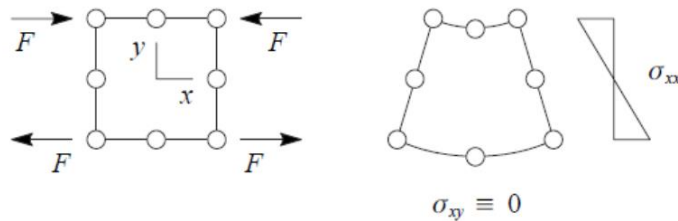
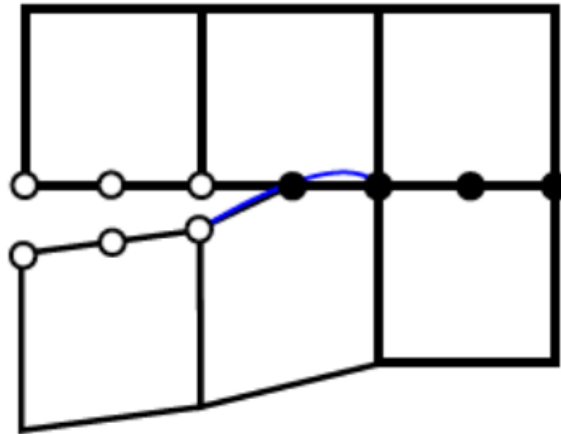


Figure 36 Deformation of a quadratic element under pure bending

The use of quadratic elements is however more important when analysing thin structures, such as beams and plates. Quadratic elements can on the other hand prove problematic when dealing with contact problems and cause the solution to converge slowly or not at all. The reason for this is the same reason why quadratic elements capture bending better than linear elements. If an edge and one corner node of an element are in contact with a surface, the quadratic interpolation of the edge shape causes a penetration of the elements. This can be seen in figure Quadratic elements should be accompanied by a surface-to-surface contact behaviour rather than a node-to-surface behaviour if they are used in a contact analysis [7].





*Figure 37 Contact between second order elements*

The meshing of this thesis is a fine mesh at the points that were needed. The element of the mesh plays a significant role in the analysis. In order to achieve the meshing, in the default section the CFD physics preference is chosen. The element order is chosen to be Quadratic and by right clicking on Mesh the Patch conforming Method and sizing are introduced. At the patch conforming method, the three bodies of gears are chosen to have Tetrahedrons and at sizing the bodies of influence is selected. There at the geometry the gears are chosen and as the bodies of influence the two cylindrical bodies are chosen. The size of elements of the bodies of influence should at least be so that 20 elements fit at the point of contact. The result of the mesh is shown in figure 38.

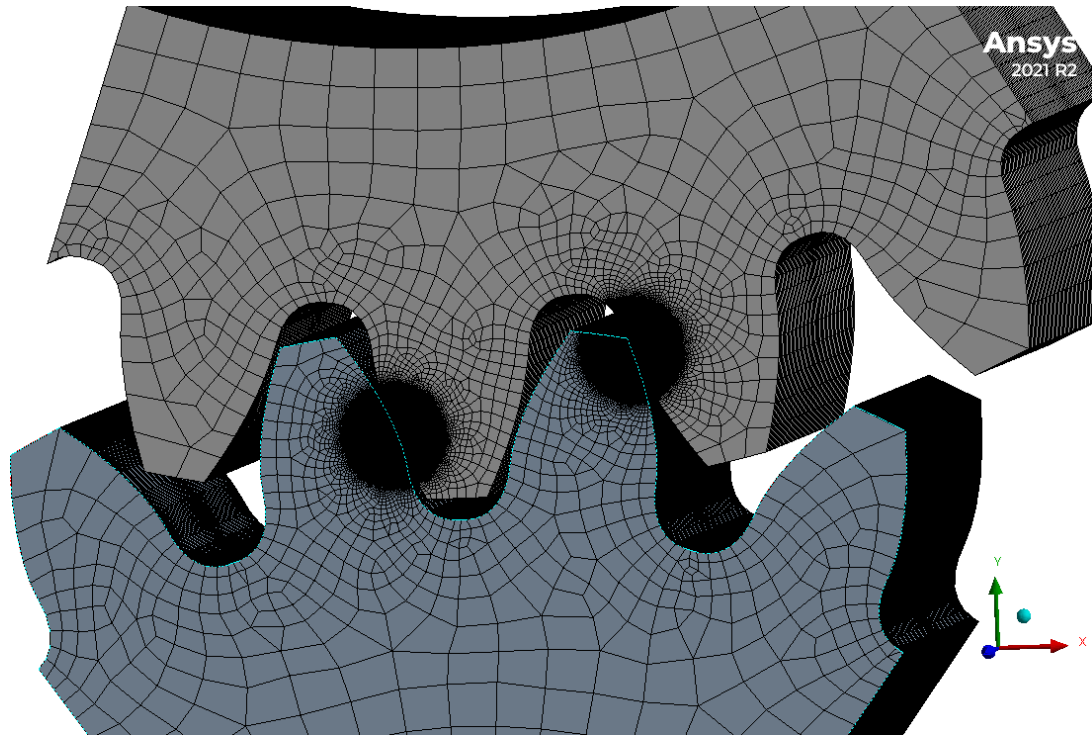


Figure 38 Final Mesh

#### 4.1.1.1.1.4 Application of Misalignment

Gears most of the time due to assembly errors develop errors such as misalignments that have significant effects on vibration, noise, strength and in this case the efficiency of the system.

The model of the peristaltic pump of this thesis appears to have significant misalignments caused by the geometry as shown before and those should be included in the model. The misalignment error of the gear shafts on the plane of action can be expressed by an inclination angle of the contact teeth on the plane of action.

In order to create those misalignments, the setting up of the simulation is similar to the previous ones. The necessary modifications that need to be made will be done in DM to create the misalignments in the assembly on purpose.

The misalignment errors in general are made using the following method. First of all from the definition of the error we know that one of the two gears-for instance here we choose the pinion-must acquire a relative angle to the other gear in the direction of the plane of action. For this purpose, a line drawn at the point of contact in position which is perpendicular to the contact trajectory of the gears which as explained previously is a line that passes from the center of the plane XY and has an incline of angle equal to  $\alpha_0$ . This line will serve as rotational axis

Secondly, by using the Rotate tool and giving as inputs the line created as axis of rotation and the value of the degrees for the angle of rotation the misalignment error is created. Now the setting up of the model can continue with the setting up of the parameters discussed in the previous paragraphs.

However, in this case this is a trivial problem which requires a  $2^\circ$  rotation around the axis.

#### 4.1.1.1.1.5 Positioning with Crowning

Crowning as explained previously is simple way to reduce the effect of misalignment both in transmission and at the contact stresses. However, it has been mentioned that in this thesis the gear profile does not have crowning, but a surface computed by MATLAB and designed in SOLIDWORKS. The modelling of the computed surface in ANSYS, is the same as crowning. As far as the setting up of the simulation is concerned it is very similar to the previous modeling as in planar spur gears.

#### 4.1.1.1.1.6 Boundary and initial Conditions

The boundary conditions that are applied were the following. Firstly, we want to prevent the pinion gear from rotating and from moving axially or radially. The latter is already fixed since the analysis is two-dimensional. The radial and rotational displacement could easily be prevented if we just fix the edge of the gear hub by using the option of Fixed Support, Displacement or Cylindrical Support. Even if this way of modelling does not make much difference in the results it is not sufficient because, we would like to fix the centre of the gear and not the edge of the hub. To do that we use the option of Remote Displacement that allows us to impose the displacement and rotation values in a Remote Point and in this case the centre of the gear, and we can select the edge of the hub to be correlated with this point. So, for the gear we set and the rotation around Z axis to be zero. For the gear in collaboration, we also set displacements along X axis and Y axis to be zero but the rotation around Z axis will be left free because in this gear the moment is applied. The boundary conditions of the two gears.

As far as the load is concerned, a moment of 60 mNm is applied in the Remote Point at the centre of the gear in collaboration. Again, the moment could also be applied directly to the edge of the hub of the gear without having much difference in the results, but this would be a less realistic way to model the problem.

#### *4.1.1.2 Modelling of involute spur gears in PGT*

In order to model the PGT of the involute spur the same method as for the pair of gears was followed only this time it was not simplified by slicing the gears but as a whole model of a planetary system. Furthermore, all the boundary and initial condition are the same as before.

Due to the misalignment induced by the pump the PGT was only tested in a misaligned analysis and for the two profiles of interest, the modified and the given profile. The rest of the analysis remains the same as before for the misaligned tests.

### 4.1.2 Transient Analysis of the PGT

#### *4.1.2.1 Modelling of the PGTs*

The transient analysis of the PGT required a different root than the one for the static analysis. First of all, this analysis requires an extra part the carrier, in contrast to the static analysis that the carrier's forces could be simulated by constraints provided by ANSYS.

Furthermore, because the material that is used is plastic, either is chosen in the material section of ANSYS or created, it requires three things. The density of the material the Young's modulus and the Poisson's ratio.

After setting up the materials for the analysis the boundary and initial conditions should take place.

#### Contacts

The transient analysis requires for all the gear teeth to mesh with each other; therefore, all the faces of each working gear should connect with the face of each gear. In order to save time and not choose each face one by one, it could be done more effectively. If the gears that first want to be connected are the sun and the one of the planets, first all the components must be hidden, except the two components of interest. Afterwards, the choosing as a target body the one that is going to be mostly deformed hide the other body and select all for the unhidden.

This will select all the faces of the existing body in this case the planet because the planet is going to be mostly deformed. After, selecting all the faces by continually pressing control deselect all the faces that do not belong to the teeth, those would be the hub and the faces of the gear. Following this method assures minimum time selecting each tooth of a gear. This is done to all the other gears as well.

Furthermore, after completing the selection process of the faces of the gears, it must be noted that the contact parameters remain the same as in the static analysis above.

However, the setting up of the connections is not finished, because the PGT requires rotation. This is achieved by inserting Joints. The joints are used on the PGT are all revolute joints which indicates the rotation of the parts. The sun gear has a revolute joint from body to ground because its rotation around a fixed center. The planet gears each one interacts with the carrier, therefore the joints of these are body to body with the carrier surfaces. Finally, the carrier as the sun gear rotates around a fixed center, therefore a joint body to ground is needed.

### Meshing

The meshing that is used is the same meshing as in the static analysis only in the transient analysis bodies of influence do not exist therefore there is no way to select different regions to mesh differently such as the contact points of the gears. However, the rest of the parameters for meshing remain the same only smaller overall elements, it should be noted that the PGT transient is computationally strenuous analysis

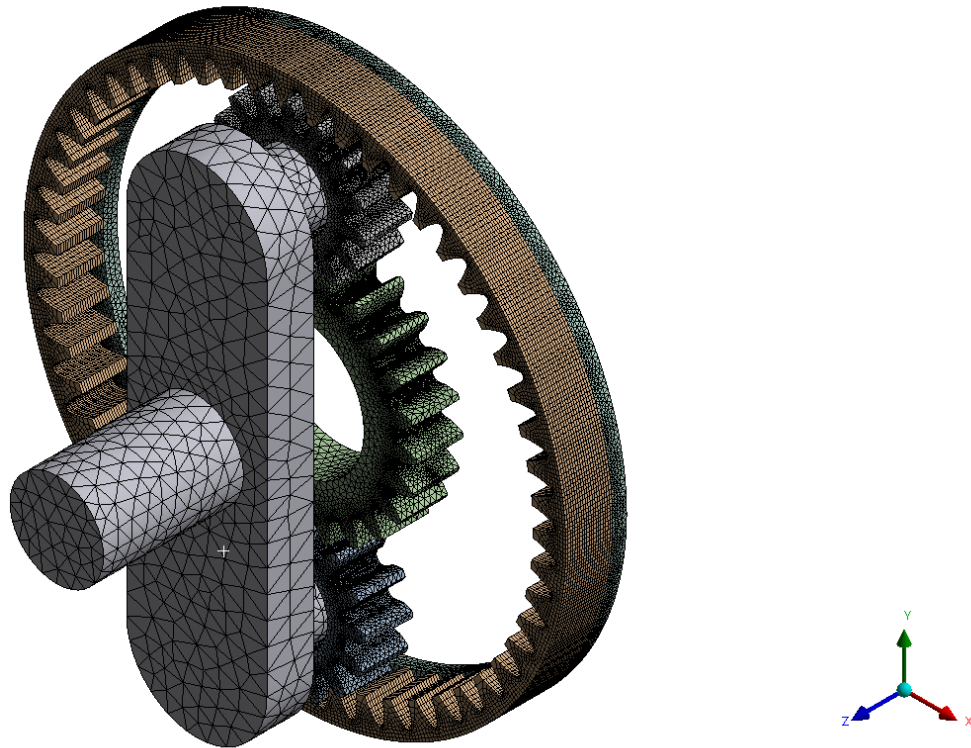


Figure 39 Meshing of the PGT in transient analysis

#### Boundary and Initial Conditions

Completing the meshing process, the initial and boundary conditions of the system should be applied. The ring of the PGT in this application remains still, therefore it was fixed in place. The planets should spin be able rotate around the sun gear in the XY plane. Therefore, a remote displacement is applied which allows the free movement and rotation except for the movement along the Z axis as they should not move up or down. Then, a joint rotation is applied in both the carrier and the sun, as the sun spin the planets and the carrier rotates the planets around the ring.

#### 4.2 Modelling of the RPC system

#### 4.2.1 Transient analysis

The RPC system transient analysis was done in order to deduce what forces and moments should be applied on the PGT in order to have a more realistic approach in its modelling. The modelling of the RPC had to take under consideration many different parameters and was a computationally strenuous problem.

The geometry was first designed in SOLIDWORKS and then inserted in DM. Afterwards, because the gears were not going to be used for the analysis, they did not matter whether they made contact or not, only for this analysis, in future studies they should be taken under consideration.

##### *4.2.1.1 Materials*

The material used for the analysis is the PVC used in all the previous analysis. Except this time the model had the tube which is made mostly of silicone. Therefore, the PGT was from PVC and the tube from silicone, both in the ANSYS material library.

##### *4.2.1.2 Contact Parameters*

The model consists of many different areas that come in contact, therefore each of the areas should be checked and selected manually due to the complexity of the model. The most important parts are the contacts of the planet-rollers with the sun-roller and the planet-rollers with the silicone tube.

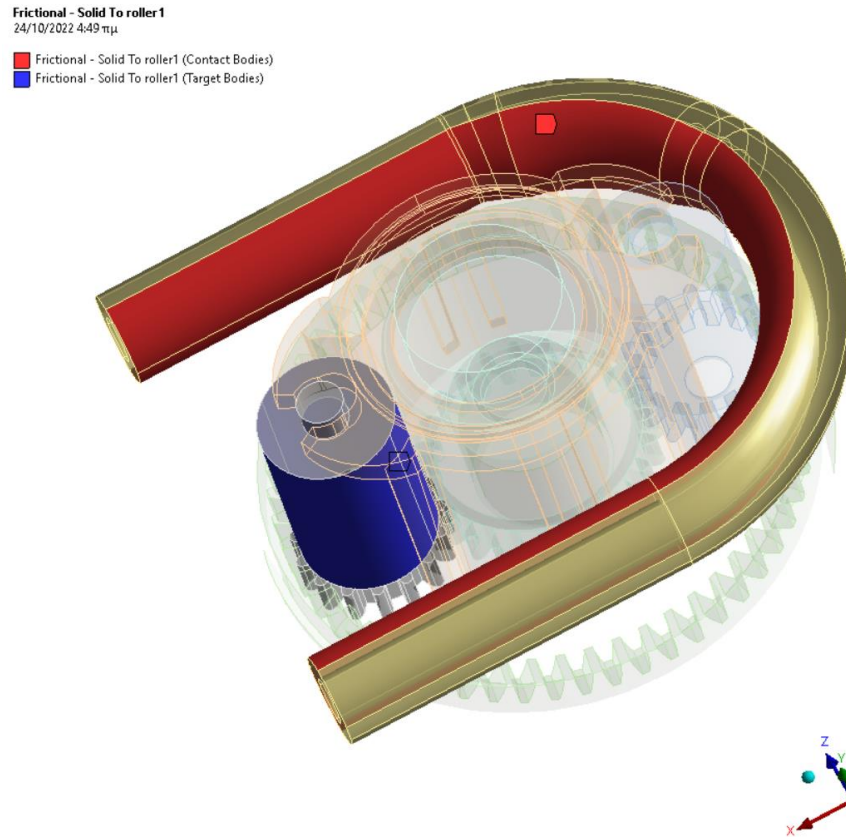


Figure 40 Frictional contact of the planet-roller with the tube

As before the joints provide the rotation for the rollers, the sun and the carrier, only this time the gears do not mesh, and a fifth joint is added which allow the tube to move in the X direction that will be useful in the initial conditions.

#### 4.2.1.3 Meshing

The complexity of the model has increased therefore the meshing should be done carefully the model provides all the meshing parameters

#### 4.2.1.4 Initial and boundary conditions

The rotations on model were applied to simulate the rotation of the gears and their effects on the compression of the tube. The remote displacements 1 and 2 are applied on the rollers of the gears to assure the free movement on the ZX plane and the spin in the Y direction. Finally,



the joint displacement is used to move the tube in its position compressing itself against the rollers.

The

**B: Transient Structural**  
Transient  
Time: 6, s  
Items: 10 of 12 indicated  
24/10/2022 4:54 πμ

- A** Joint - Rotation: 936, °
- B** Joint - Rotation: -936, °
- C** Joint - Rotation: -936, °
- D** Fixed Support
- E** Remote Displacement
- F** Remote Displacement 2
- G** Remote Displacement 3
- H** Joint - Rotation: 288, °
- I** Joint - Displacement: 2, mm

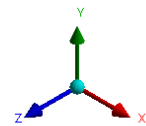
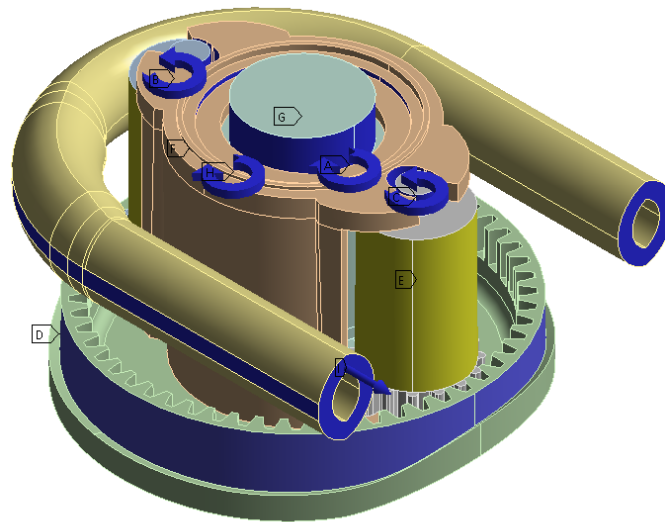


Figure 41 Initial and boundary conditions for the RPC

## 5. Results

In this chapter the results of the tests that run will be examined and discussed. Completing the modelling process as well as understanding the theoretical background of the problems tackled in this thesis, the tests were set in motion. The results are used in order to examine whether the code produces a better profile than the involute profile in the presence of misalignments and to determine whether this optimal profile is better than the existing one. Furthermore, the results compare the theoretical model of the RPC [8] with a more realistic version of it. Finally, it used to determine whether the profiles in the PGT

### 5.1. Analysis of cylindrical gear pair and PGT

#### 5.1.1 Static Structural Analysis

These tests run with consistent initial conditions such as the meshing and the moment applied to the gears, as well as the boundary conditions that have been explained in the previous chapter. The initial conditions of each test will be shown for a better overview of the whole process.

TABLE WITH THE INITIAL CONDITIONS for the statics

*Table 1 General Characteristic for  $m=1.5$*

z1	25
z2	20
ao(°)	20
xerr(°)	2
moment(Nmm)	-60

##### 5.1.1.1 Test 1 Involute Profile $m=1.5$

In the following test the involute profile generated by KISSSOFT is being used and examined both as a control and a comparison for the rest of the tests.

As it can be seen the deformation of the gear as well as the contact stresses follow the pattern that was established before in the other studies. The plastic gear does not follow the Hertz Theory as well as its metallic counterpart. Plastic gears show lesser stresses than the ones calculated by Hertz theory and this can be shown below.

### 5.1.1.1.1 Deformation

The deformation of the gear is highest at the teeth of the driven gear, as it is going to experience the moment from the driver gear and as it is fixed at the hub, its teeth will deform.

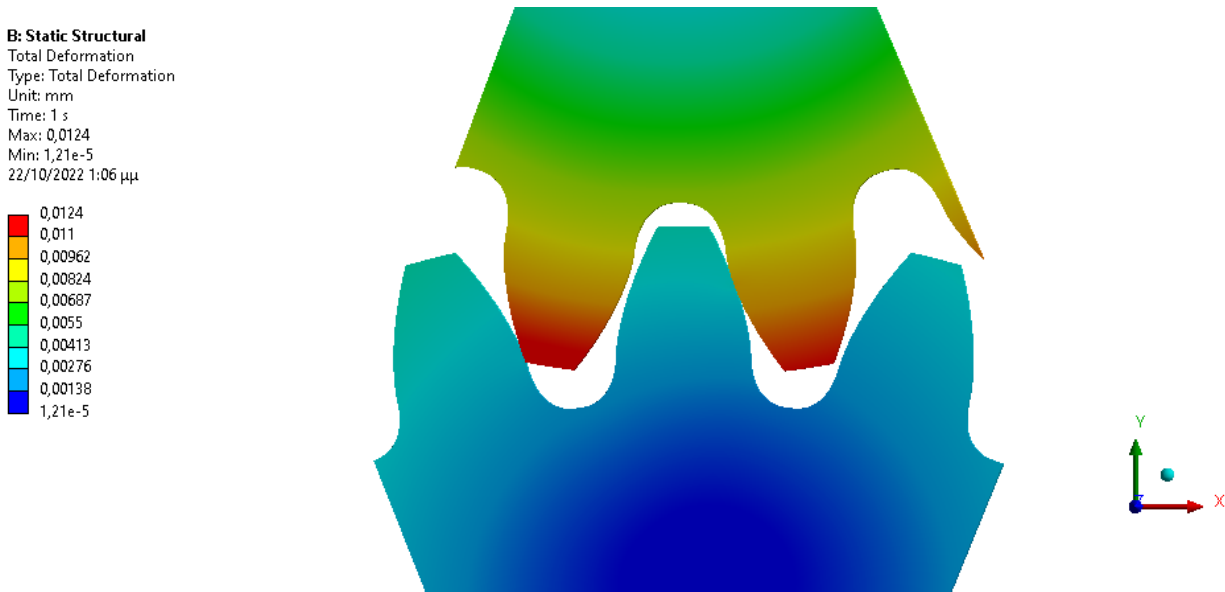


Figure 42 Frontal view of deformation

### 5.1.1.1.2 Equivalent Von Misses stress

The stresses that develop on the surface of the teeth for each gear create a parabolic pattern as it can be seen at it's of the contact points of each gear. The stresses do not follow the Hertz theory as they are lesser than it is estimated by the theory, as shown in table 123 and the following pictures.

**B: Static Structural**

Equivalent Stress  
 Type: Equivalent (von-Mises) Stress  
 Unit: MPa  
 Time: 1 s  
 Max: 8,1257  
 Min: 0,00028157  
 22/10/2022 1:06 μμ

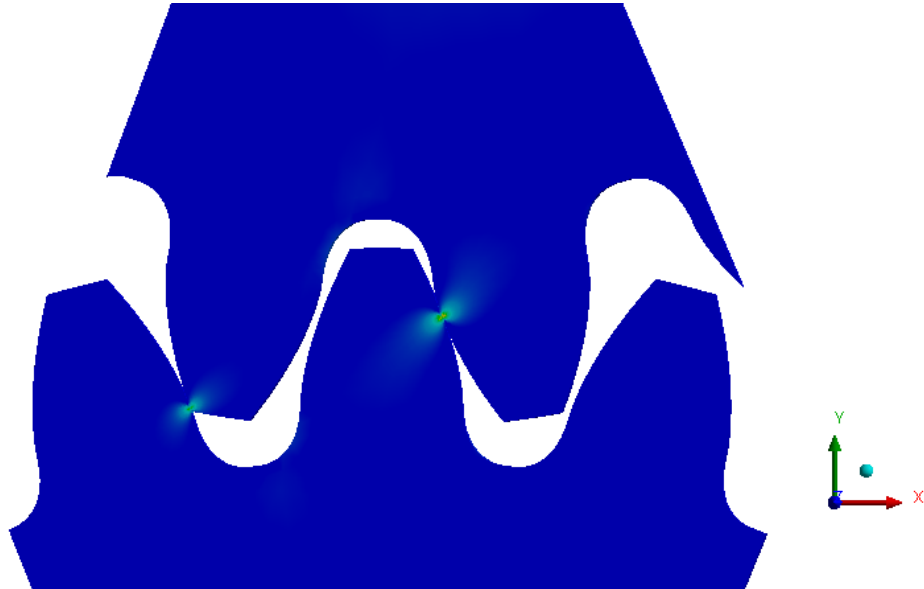
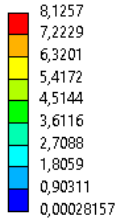


Figure 43 Equivalent von-Mises Stress frontal

## TABLE

#### 5.1.1.1 Test 2 Modified Involute Profile $m=1.5$

For the second test the modified profile was used to compare it with the involute profile. As it can be seen the optimal profile has reduced deformation compared to the involute profile and the contact stresses focusing them only on a point of the gear and not the whole tooth, as it was desired. Therefore, the MATLAB code worked for the first part. However, this has only proven its workability at a planar level further testing is done in order to ascertain its capability with misalignments.

#### 5.1.1.1.3 Deformation

The deformation of the modified gear profile is similar to the normal involute profile and that is to be expected, as the point at which makes contact is the same as in the involute profile due to the nature of the code.

**B: Static Structural**  
Total Deformation  
Type: Total Deformation  
Unit: mm  
Time: 1 s  
Max: 0.0172  
Min: 4.58e-5  
23/10/2022 6:03 πμ

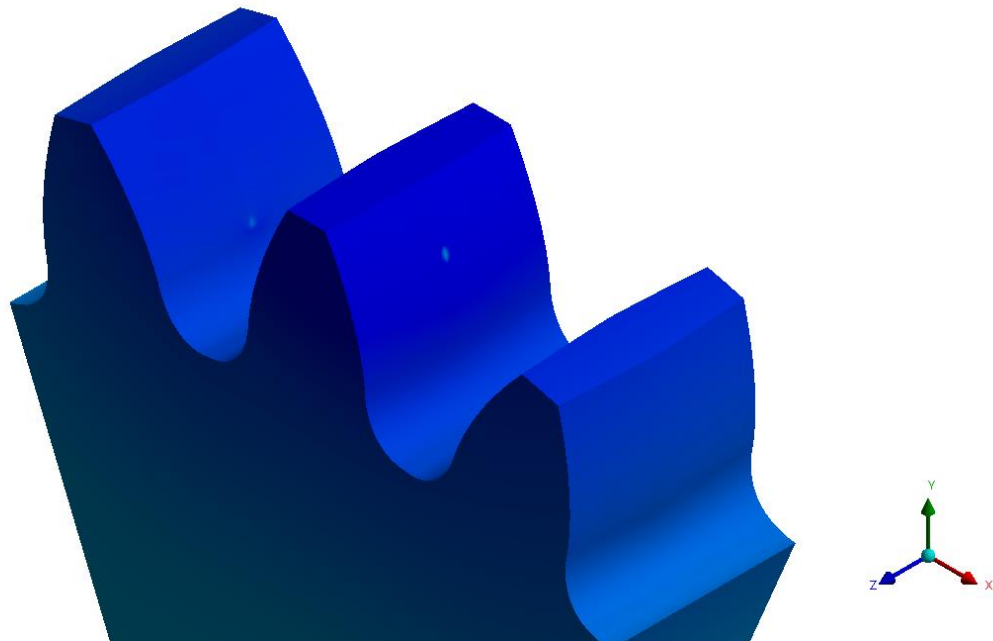
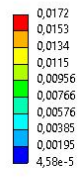


Figure 44 Deformation of the driver gear

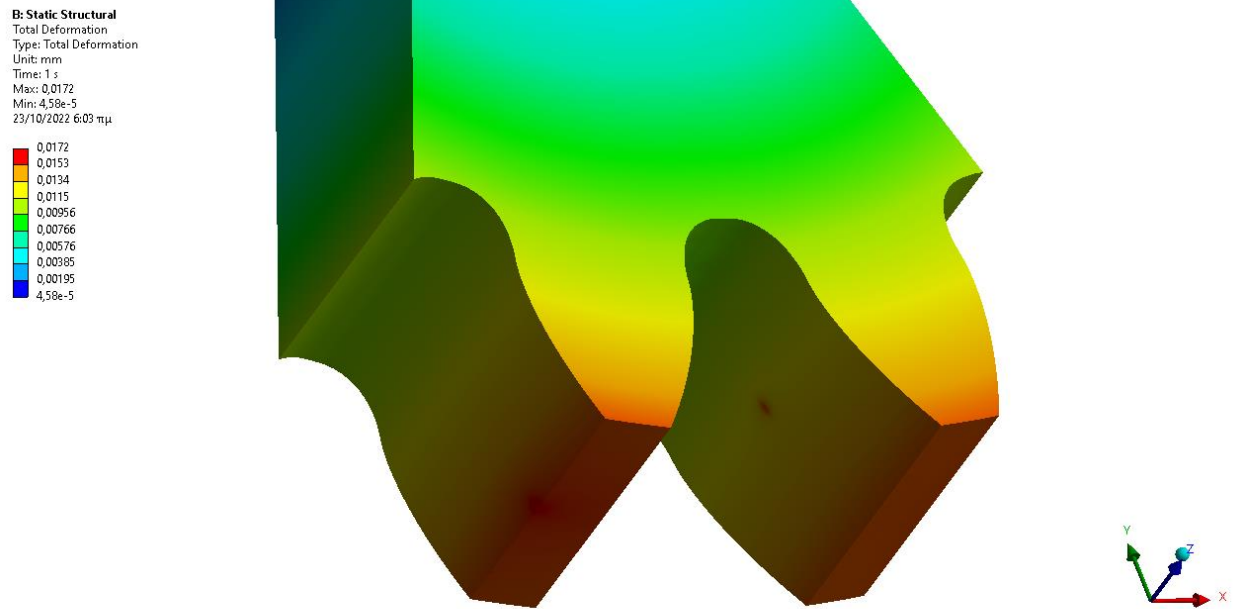


Figure 45 Deformation of the driven gear

However, the contact stresses are far greater than the ones at the involute profile. This is since the modified profile has a singular point at its whole facewidth, where the involute profile could distribute the pressure more evenly along the whole tooth. This was expected for the involute to outperform the modified profile in planar testing.

#### 5.1.1.1.4 Equivalent Von Misses stress

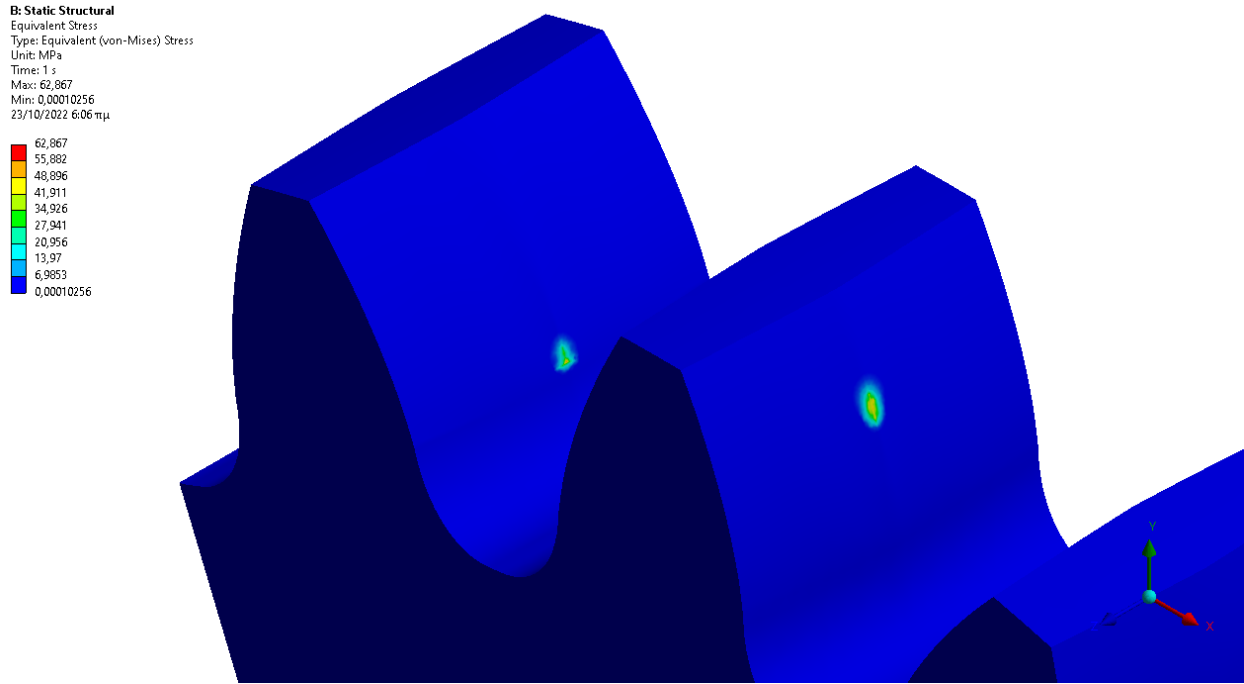


Figure 46 Equivalent von Misses stress of the driver gear

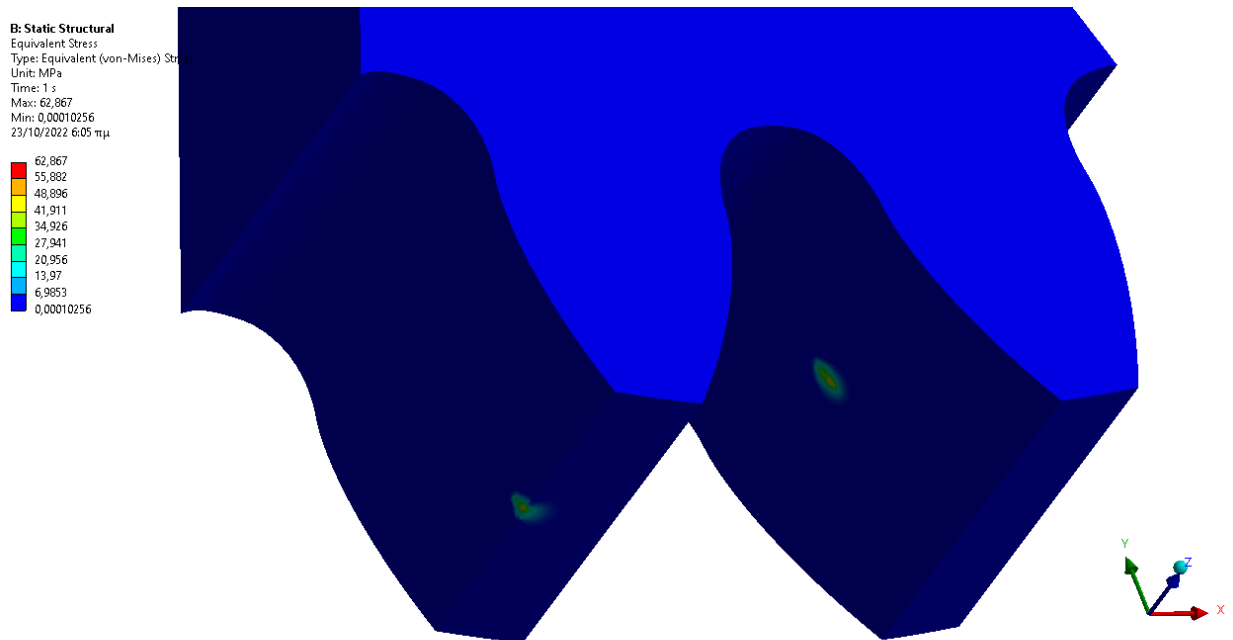


Figure 47 Equivalent von Misses stress of the driven gear

### 5.1.1.1 Test 3 Involute Profile $m=1.5$ with $2^\circ$ misalignment along the Y axis

After completing the benchmark tests to ensure that the involute was working correctly and the optimal profile as well. Then the gears were tested with misalignments set up as it was explained above.

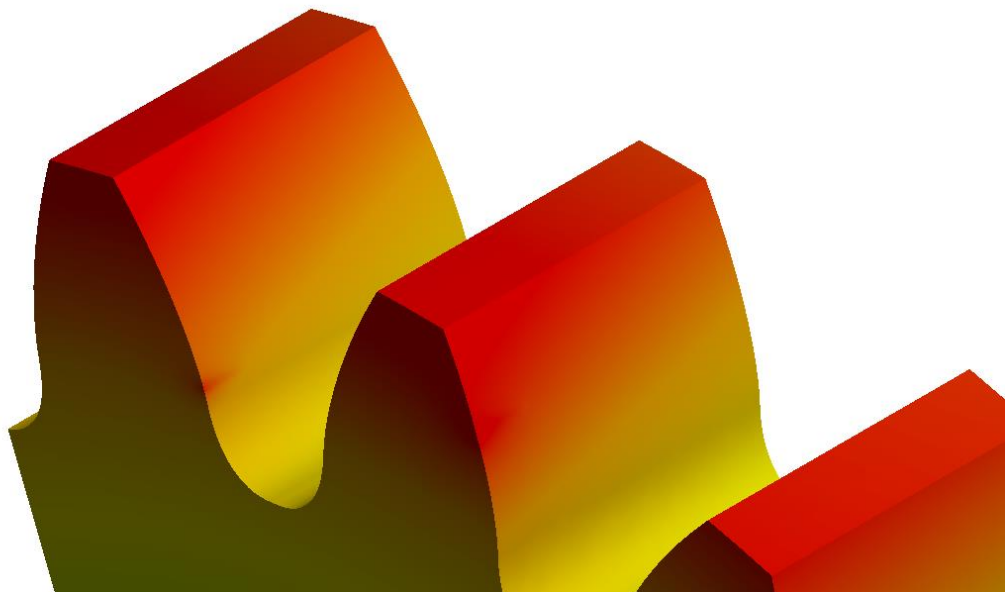
With the following test it can be observed that the involute with misalignment produces contact stresses at a certain point of the tooth more specifically its edge. Due to the triviality of the problem the induced misalignment was  $2^\circ$  along the Y axis as explained. The misalignment is the center of this thesis due to its appearance at the application of the peristaltic pump. Therefore, it was natural to examine the gears with this misalignment.

The deformation of the gear follows the expected pattern as it has deformed most at the edge of the tooth at as it moves further from the contact point there is less deformation.

#### 5.1.1.1.5 Deformation

**B: Static Structural**  
Total Deformation  
Type: Total Deformation  
Unit: mm  
Time: 1 s  
Max: 0,0381  
Min: 2,12e-5  
14/10/2022 4:00 μμ

0,0381
0,0339
0,0296
0,0254
0,0212
0,0169
0,0127
0,00848
0,00425
2,12e-5





## DEFORM OF THE DRIVEN GEAR

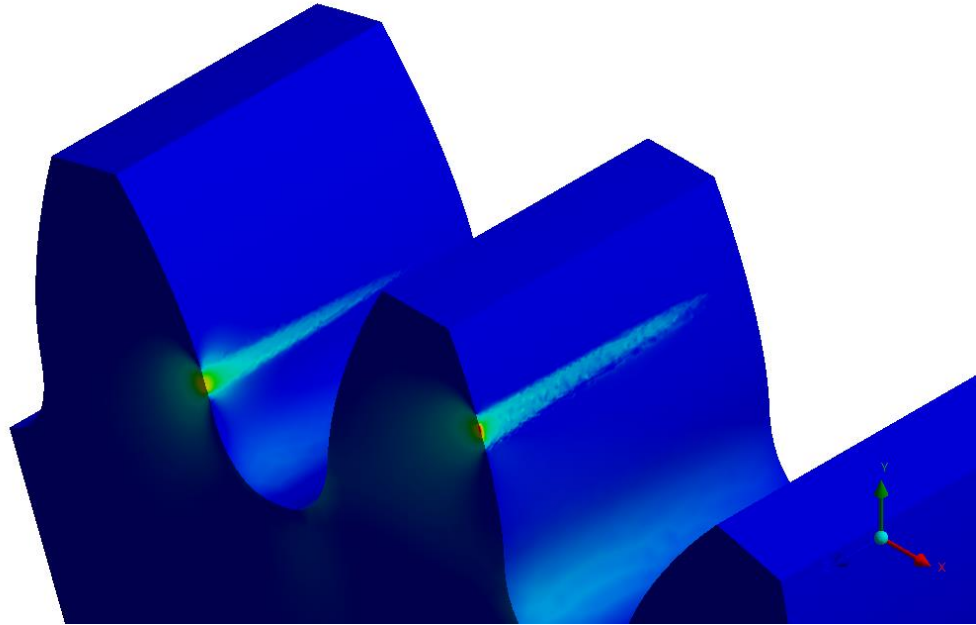
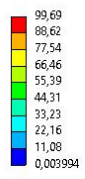


The contact stresses follow the same pattern as it was described in the previous chapters.

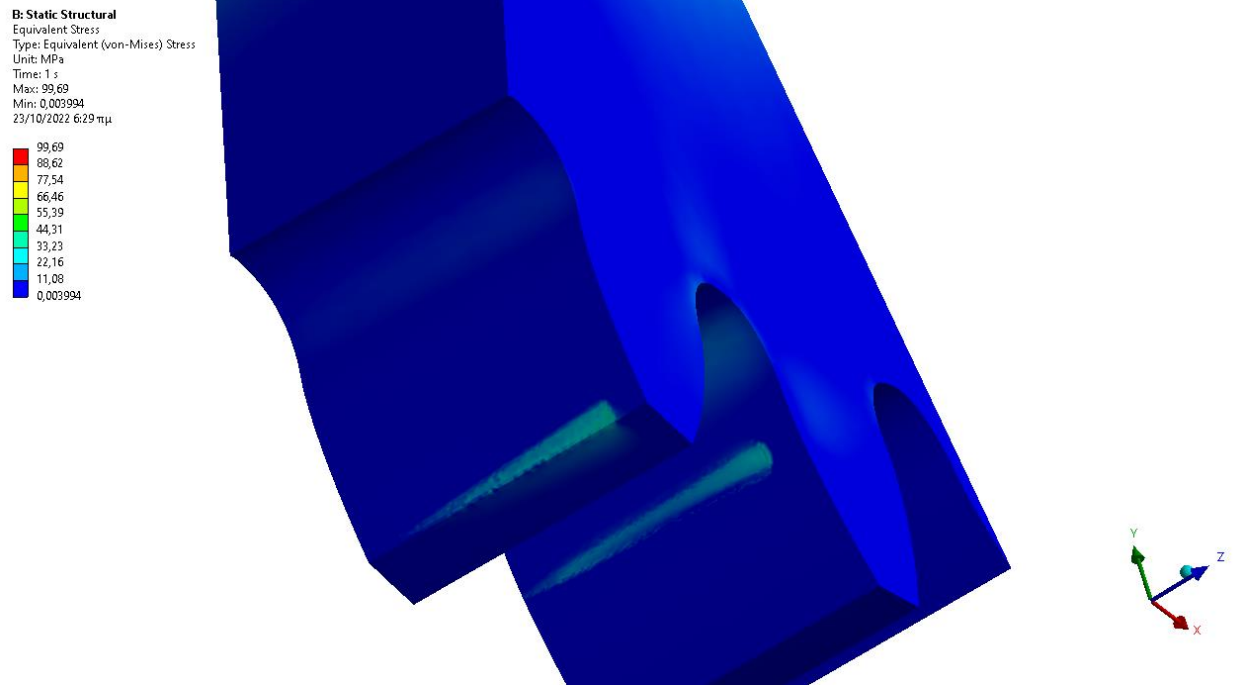
## 5.1.1.1.6 Equivalent Von Misses stress

## VON MISSES OF THE DRIVER

**B: Static Structural**  
Equivalent Stress  
Type: Equivalent (von-Mises) Stress  
Unit: MPa  
Time: 1 s  
Max: 99,69  
Min: 0,003994  
23/10/2022 6:29 πμ



### VON MISSES OF THE DRIVEN

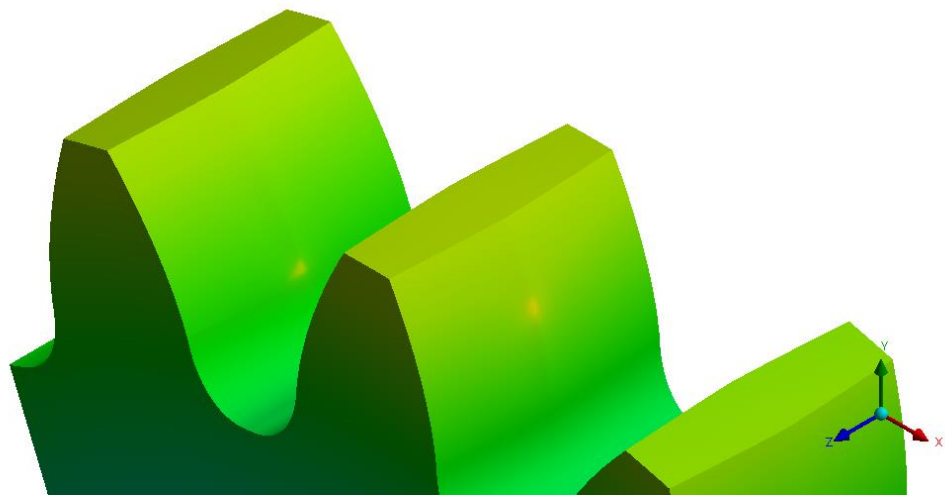
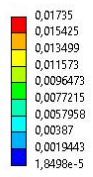


#### 5.1.1.1 Test 4 Modified Involute Profile $m=1.5$ with $2^\circ$ misalignment along the Y axis

The results from the involute profile with and without misalignment followed the predictable pattern, when misaligned it showed five times worst behavior in contact stresses and three times worst behavior at the de

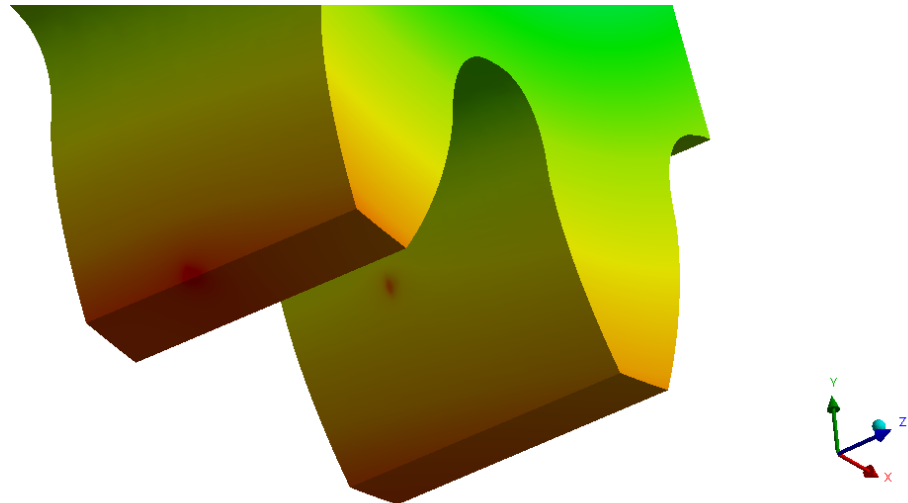
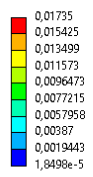
#### 5.1.1.1.7 Deformation

**B: Static Structural**  
 Total Deformation  
 Type: Total Deformation  
 Unit: mm  
 Time: 1 s  
 Max: 0,01735  
 Min: 1,8498e-5  
 23/10/2022 9:40 μμ



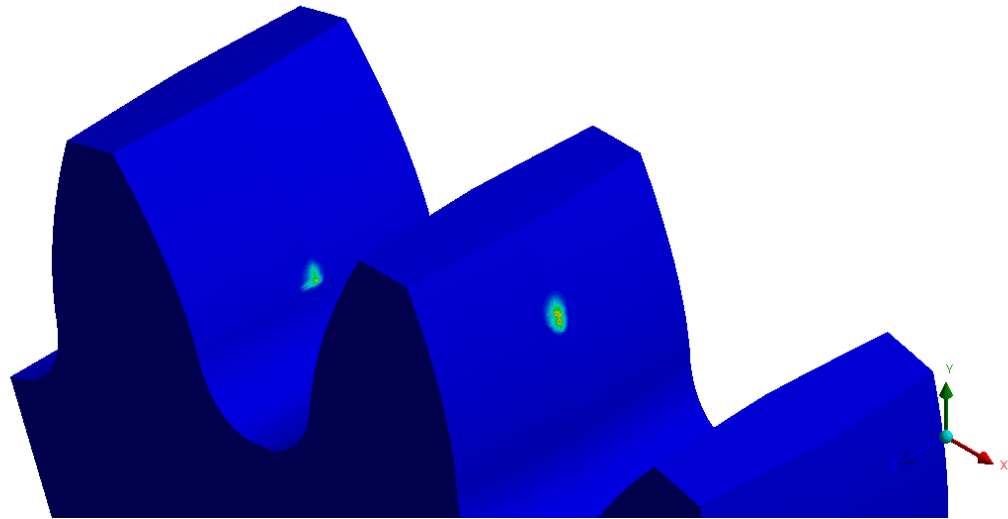
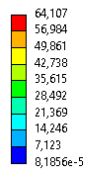
### DEFORM OF THE DRIVEN GEAR

**B: Static Structural**  
 Total Deformation  
 Type: Total Deformation  
 Unit: mm  
 Time: 1 s  
 Max: 0,01735  
 Min: 1,8498e-5  
 23/10/2022 9:40 μμ



### 5.1.1.1.8 Equivalent Von Misses stress

**B: Static Structural**  
Equivalent Stress  
Type: Equivalent (von-Mises) Stress  
Unit: MPa  
Time: 1 s  
Max: 64,107  
Min: 8,1856e-5  
23/10/2022 9:41 μμ



VON MISES DRIVEN

**B: Static Structural**  
Equivalent Stress  
Type: Equivalent (von-Mises) Stress  
Unit: MPa  
Time: 1 s  
Max: 64,107  
Min: 8,1856e-5  
23/10/2022 9:41 μμ

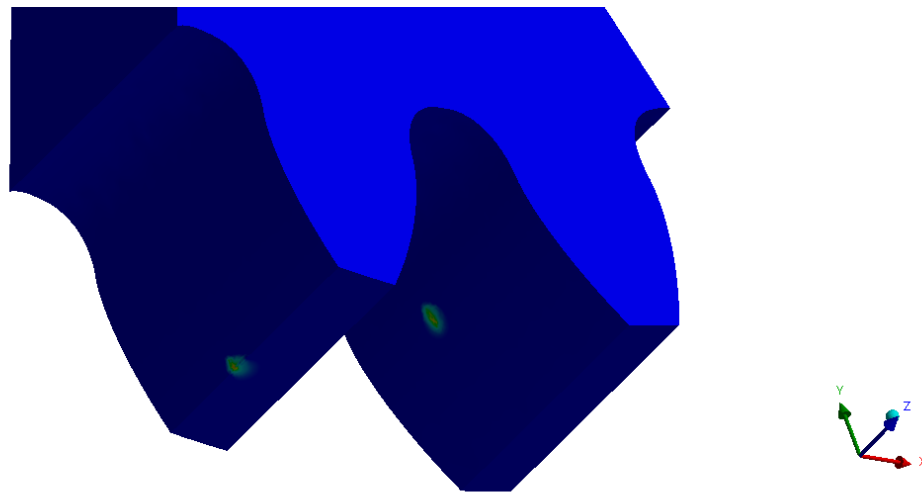
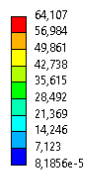


Table 2 General Characteristics for  $m=0.4$ 

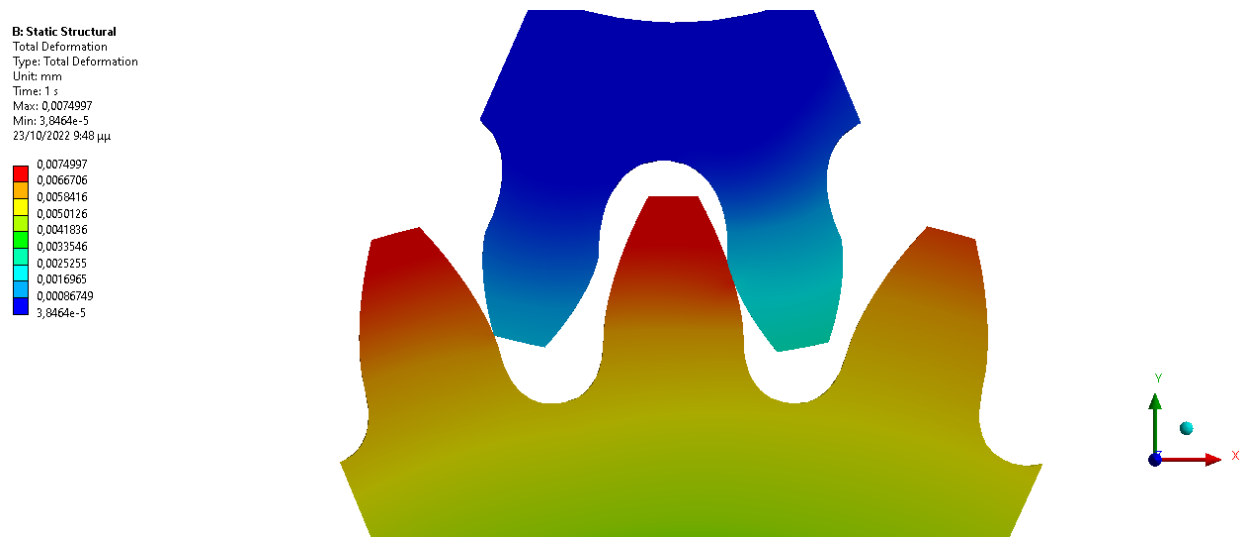
z1	15
z2	24
ao(°)	20
xerr(°)	2
moment(Nmm)	-6

#### 5.1.1.1 Test 5 Involute Profile $m=0.4$

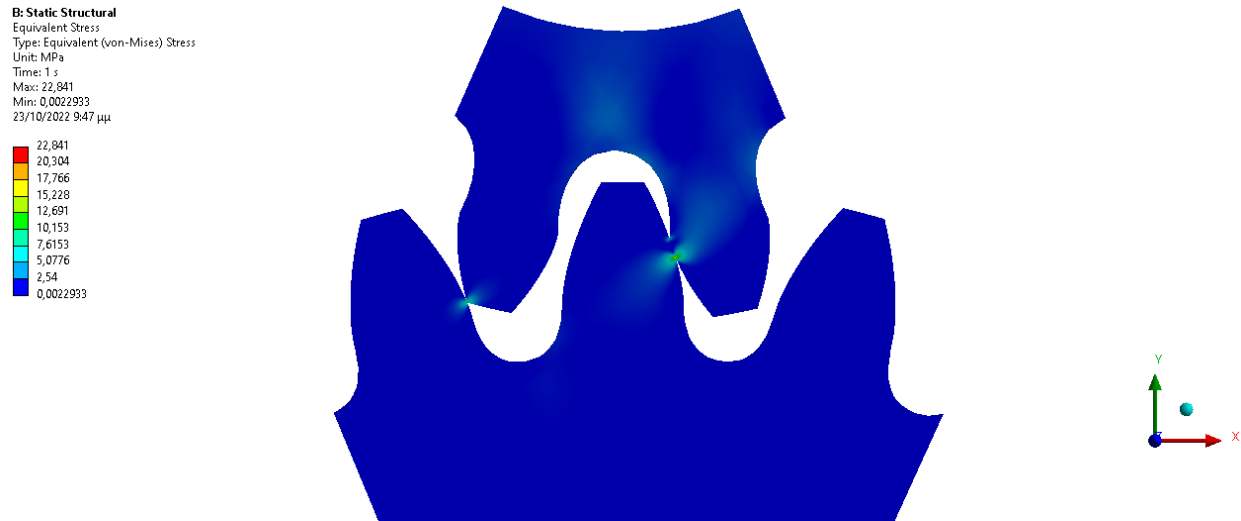
This test was done in order to have a benchmark test. The involute profile follows already established rules therefore, it must be tested so it can be compared with the rest of the unknown profiles.

##### 5.1.1.1.9 Deformation

The deformation is similar to the deformation of the previous gear with different module as it was expected. The contact stresses behave the same way as well.



##### 5.1.1.1.10 Equivalent Von Misses stress



VON MISSES DRIVER

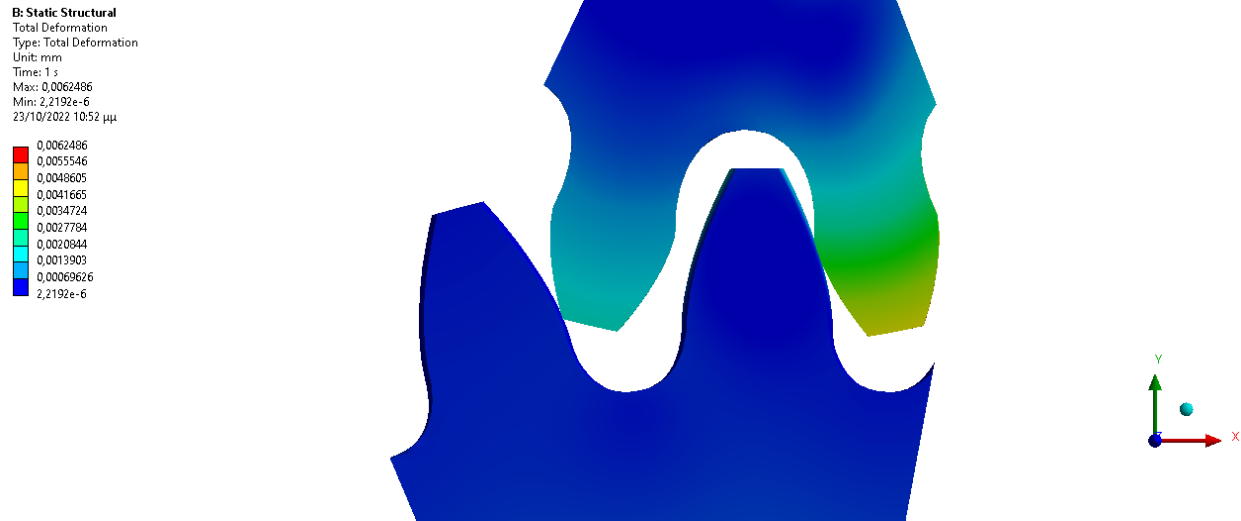
VON MISSES DRIVEN

#### 5.1.1.1 Test 6 Modified Involute Profile $m=0.4$

The modified profile tested first a planar level is another benchmark test that helps to assure both that the previous test was done correctly and gave the same results and so that it can be compared to other profiles.

The deformation of the modified profile follows the same pattern as with the other module, which is encouraging proving that it can be scaled up and down and that the designing process was done correctly and consistently for both modules. The contact stresses as expected all concentrate in a point in the center as it should according to the previous tests.

#### 5.1.1.1.11 Deformation



DEFORM OF THE DRIVER GEAR

DEFORM OF THE DRIVEN GEAR

#### 5.1.1.1.12 Equivalent Von Misses stress

VON MISSES DRIVER

VON MISSES DRIVEN

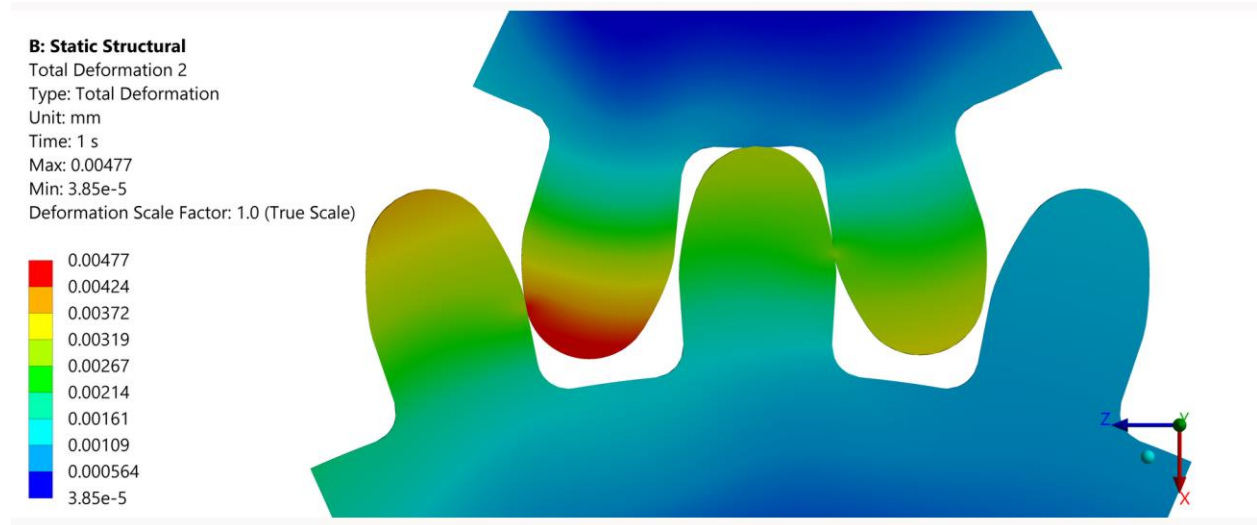
#### 5.1.1.1 Test 7 Given Profile $m=0.4$

The profile used in this application does not resemble the involute profile nor any other similar profile. It can be assumed that it was an involute profile modified as well in order to better fit the mechanism it is in because of the great misalignments. However, because it is not surely an involute and this can be seen because when there is distance between the gears the degree of overlap falls dramatically. Then it is an unknown profile.

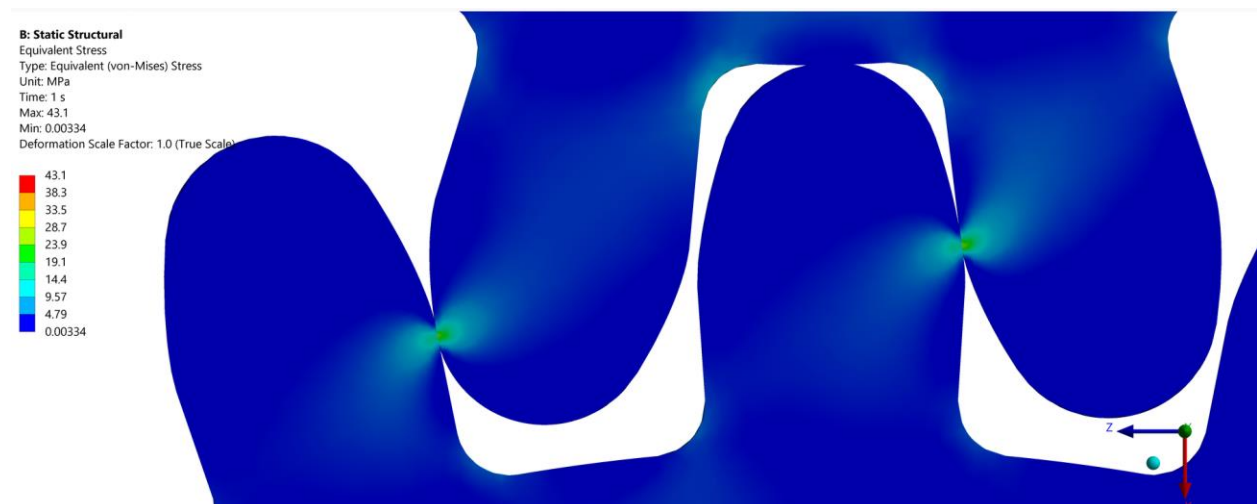


The deformation and the contact stresses of the profile are calculated using the FEM analysis and the results are shown below.

#### 5.1.1.1.13 Deformation

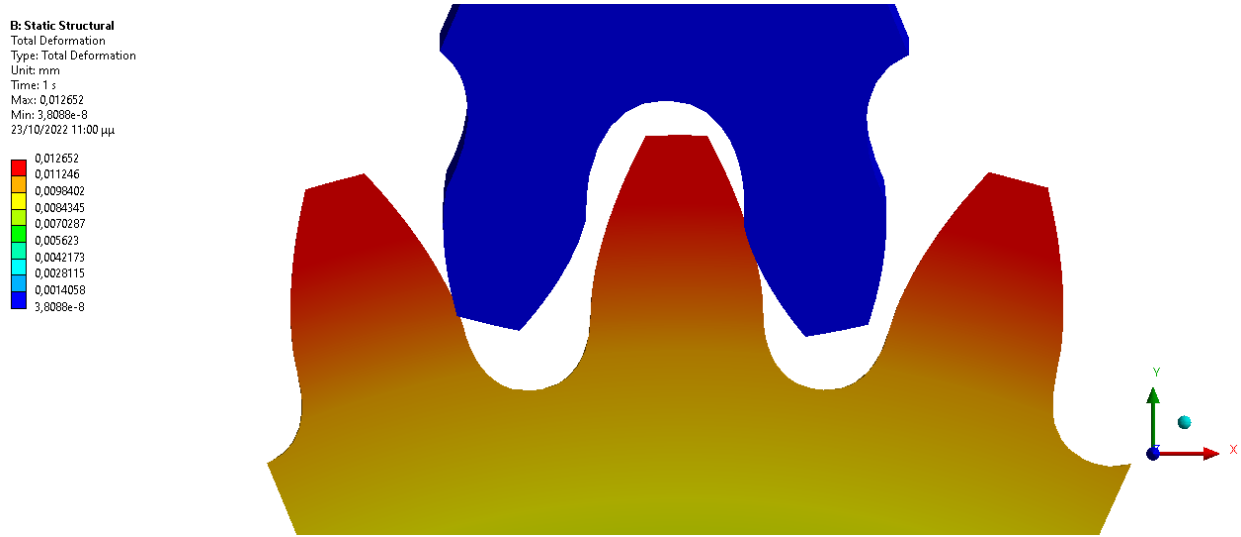


#### 5.1.1.1.14 Equivalent Von Mises stress

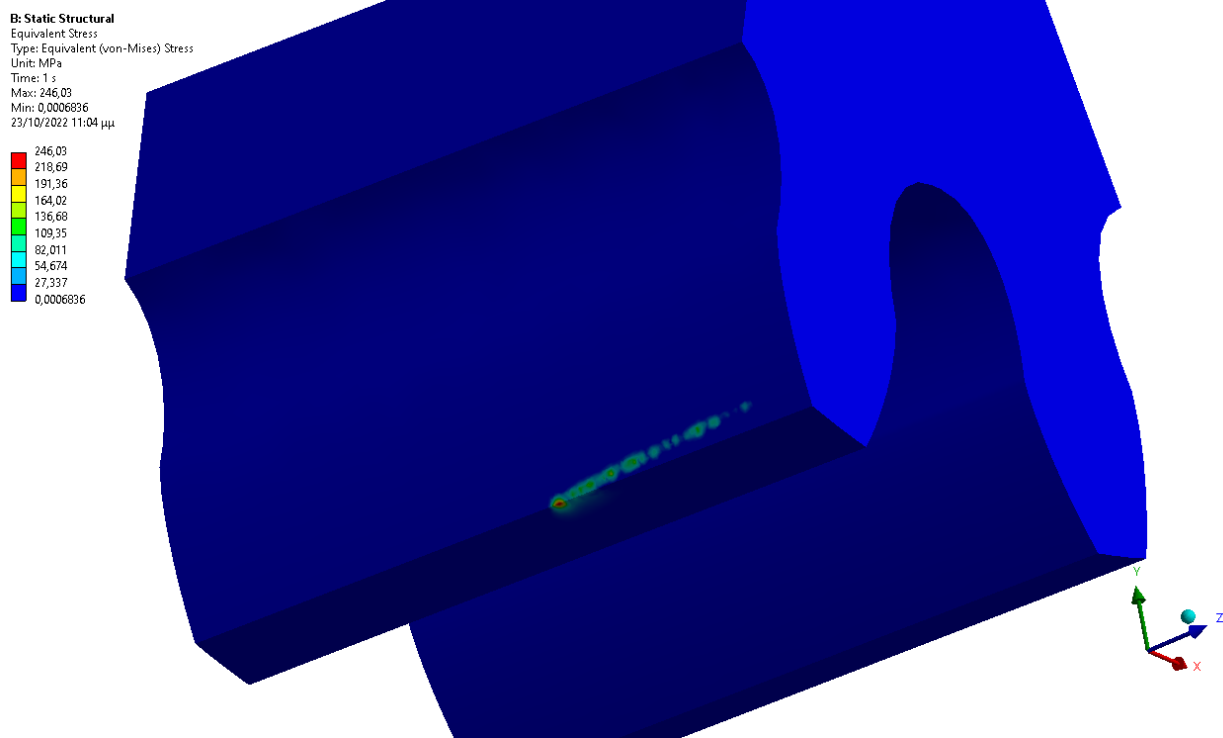


5.1.1.1.1 Test 8 Involute Profile  $m=0.4$  with  $2^\circ$  misalignment along the Y axis

5.1.1.1.15 Deformation



5.1.1.1.16 Equivalent Von Misses stress



### 5.1.1.1 Test 9 Modified Involute Profile $m=0.4$ with $2^\circ$ misalignment along the Y axis

#### 5.1.1.1.17 Deformation

#### 5.1.1.1.18 Equivalent Von Misses stress

### 5.1.1.1 Test 10 Given Profiles with $2^\circ$ misalignment along the Y axis

#### 5.1.1.1.19 Deformation

**B: Static Structural**

Total Deformation

Type: Total Deformation

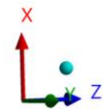
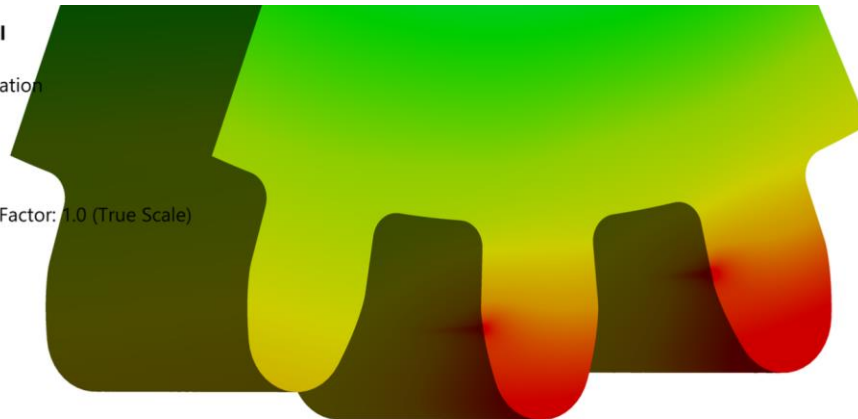
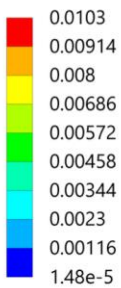
Unit: mm

Time: 1 s

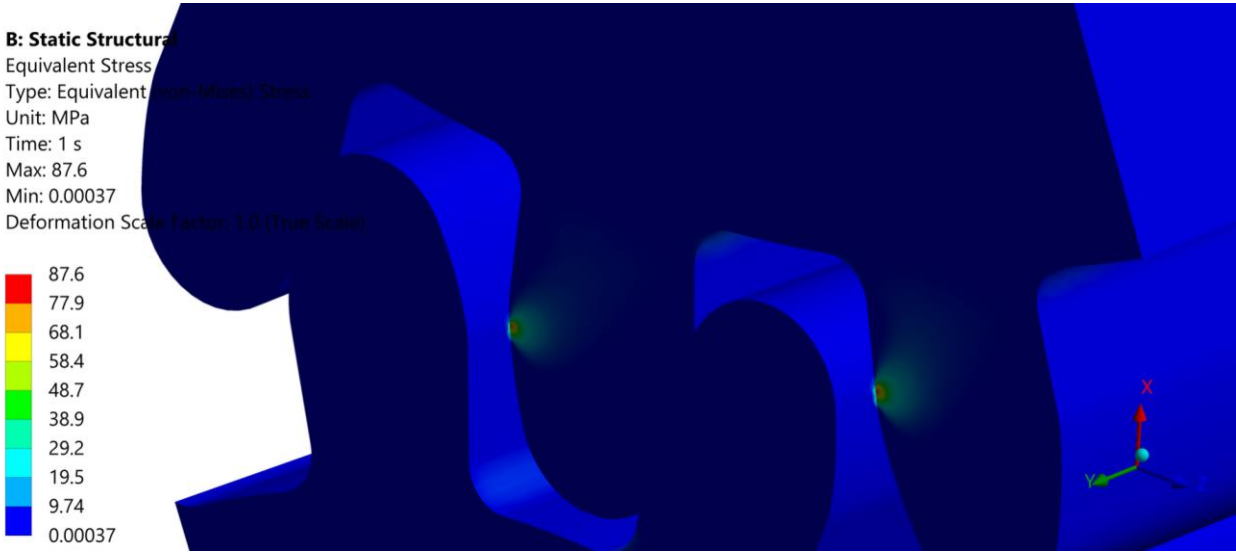
Max: 0.0103

Min: 1.48e-5

Deformation Scale Factor: 1.0 (True Scale)



#### 5.1.1.1.20 Equivalent Von Misses stress



5.1.2 Comparison of the one-stage gear pairs

5.1.2.1 Profiles  $m=1.5$

As it can be seen the behavior of the modified involute profile in the presence of misalignments is linear compared to the behavior of the involute profile which increases as expected from the bibliography

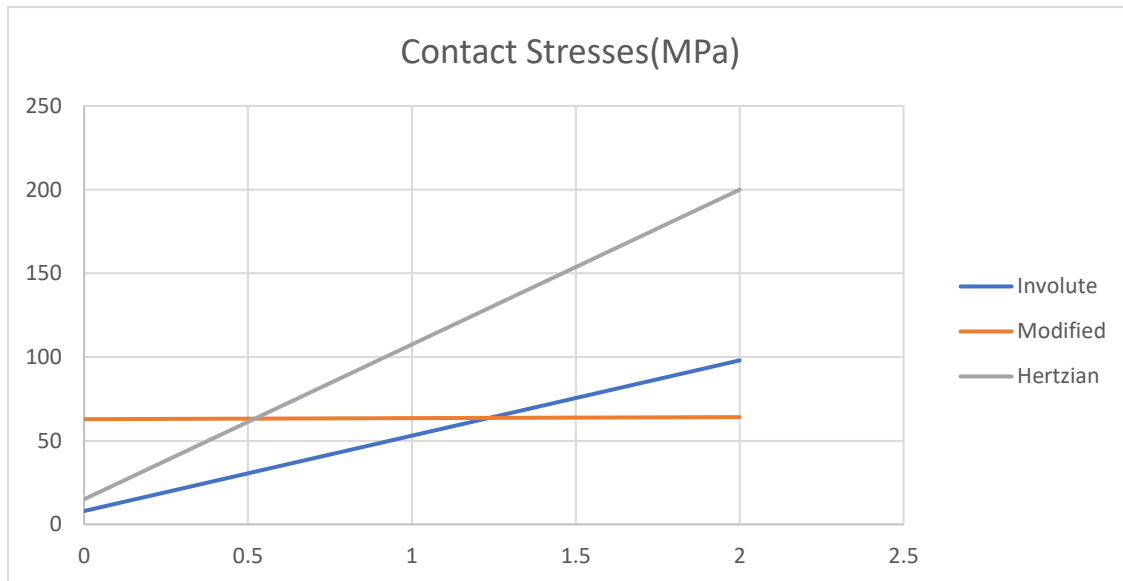


Chart 1 Comparison of contact stresses for  $m=1.5$

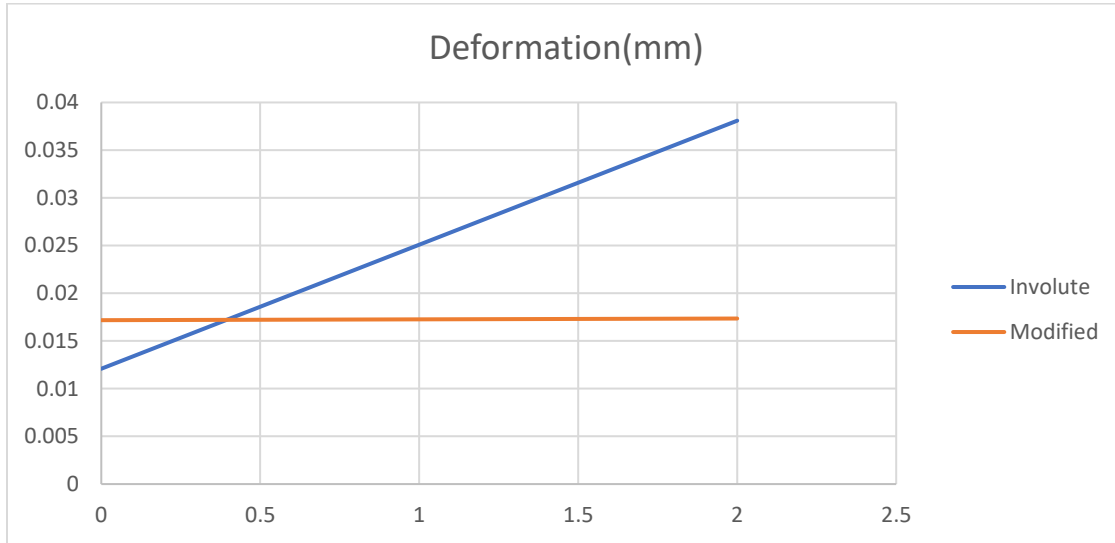


Chart 2 Comparison of deformation of m=1.5

No Misalignment			
Results			
	Test1	Test2	
	Normal profile	Modified profile(z2)	Comparison(%)
<b>Total Deformation(mm)</b>	0.012088	0.017178	0.296309233
<b>Von misses(MPa)</b>	8	62.867	
<b>mesh(#of elements)</b>	402679	568586	
Hertz	15		

5.1.2.2 Profiles  $m=0.4$

Misalignment				
Results				
		Test3	Test4	
		Normal profile	Modified profile(z2)	Comparison(%)
Total Deformation	(mm)	0.038088	0.01735	0.54447595
Von misses	(MPa)	98	64.107	
mesh(#of elements)		388975	559546	
Herzt	(MPa)	200		

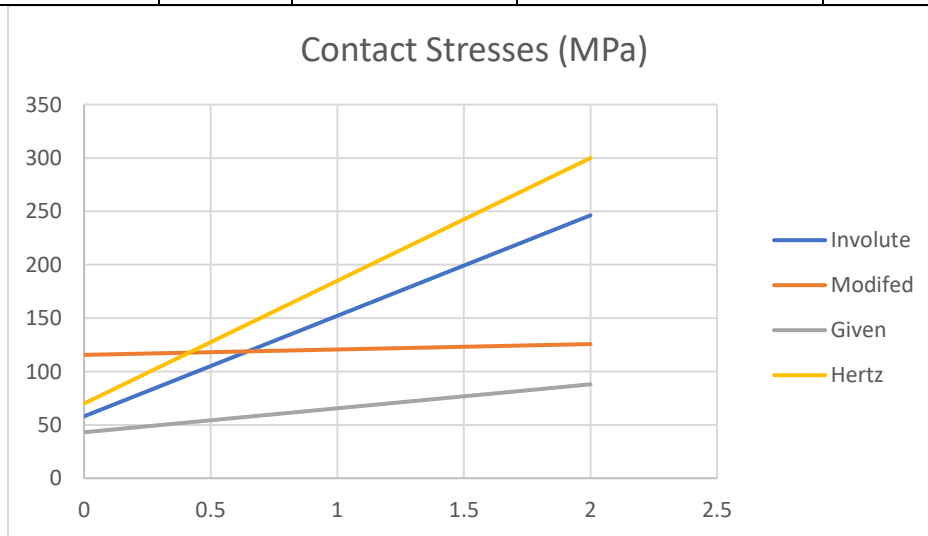


Chart 3 Contact stresses for  $m=0.4$

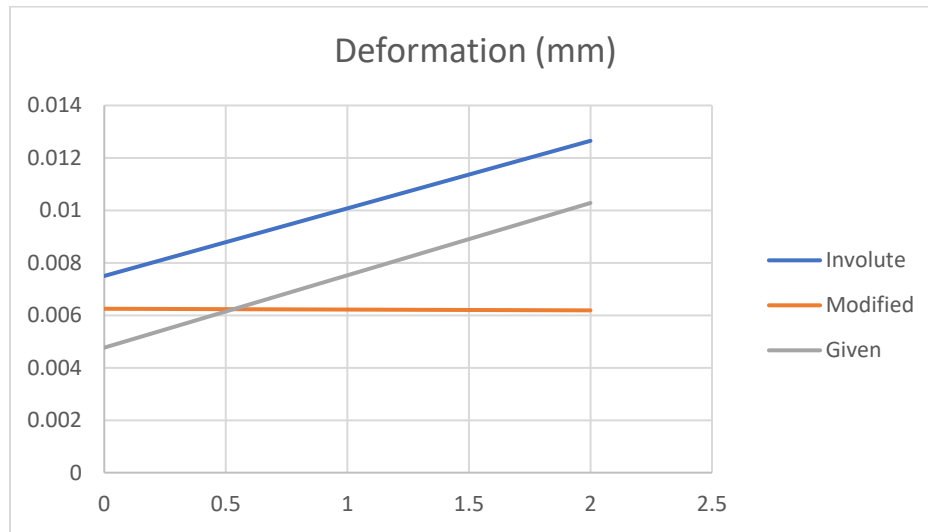


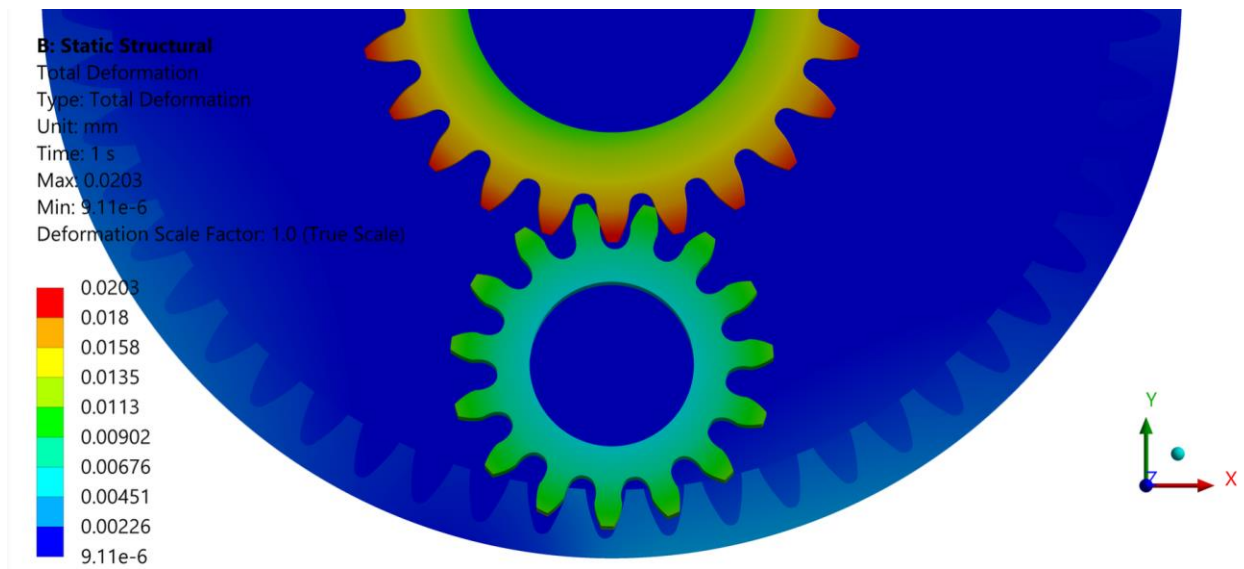
Chart 4 Deformation for  $m=0.4$

Summarizing the results in the tables and diagrams there are some conclusions that can be drawn. The involute profile follows the established theory in the bibliography both at the planar and at the misaligned testing and performs the worst. The unknown profile used in the application performs better than the involute in the contact stresses and deformation, however its degree of overlap is very low as it is and when there is greater distance between the gears the transmission will be suboptimal at best. Finally, the modified optimal profile performs the best both at the planar and the misaligned testing. Those are very encouraging results as it can work as a proof of concept for the method developed in the MD LAB. However, due to limiting the testing only at a certain misalignment with certain moments applied to the gear, solid conclusions cannot be drawn, but further investigating should provide the necessary data to establish this method for producing profiles fitted for misalignments.

### 5.1.3 PGT test with Modified Involute Profile with $2^\circ$ misalignment along the Y axis

After the results as a pair of gears the application demands that they should provide better results in the PGT as well. Testing the model yielded fruitful results as it can be seen with deformation and the contact stresses in the figure 123.

#### *Deformation*



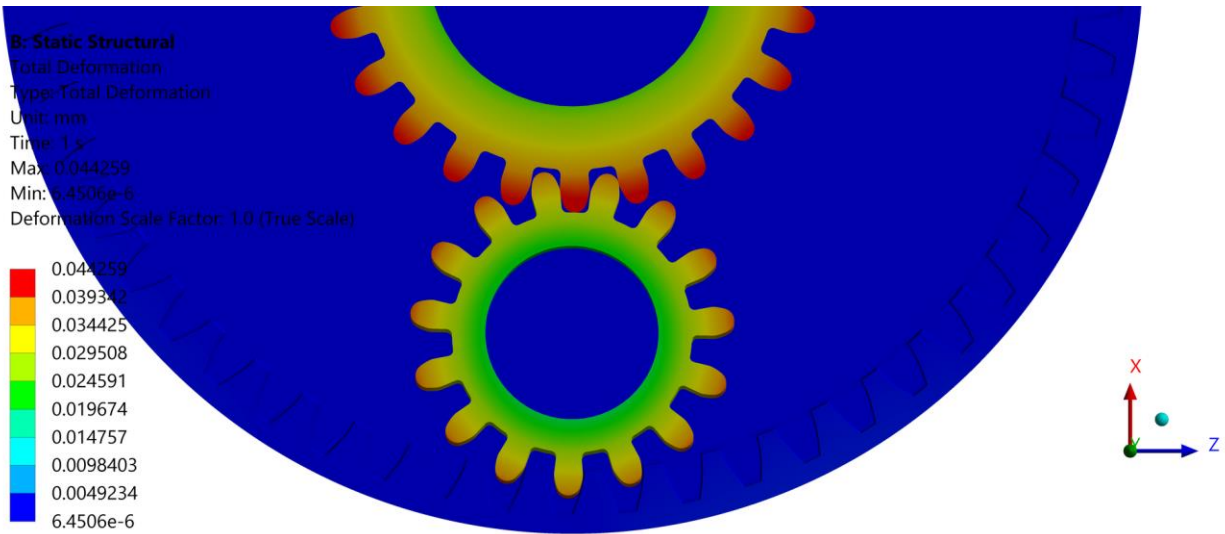
*Equivalent Von mises stress*

Picture in desktop ntua

5.1.4 PGT test with Given Profile with 2° misalignment along the Y axis

*5.1.4.1 Deformation*





5.1.4.2 Equivalent Von mises stress

Picture in desktop ntua

5.1.5 Comparison of the PGT systems

From the comparison of the two PGTs it can be seen that the modified PGT yielded better results both in the contact stresses and the deformation.

		Modified profile	Given	Comparison(%)
Total Deformation(mm)		0.0202	0.044259	54.40%
Von mises(MPa)		22	106.42	
mesh(#of elements)		2394929	5200000	

5.1.6 Transient of the PGT

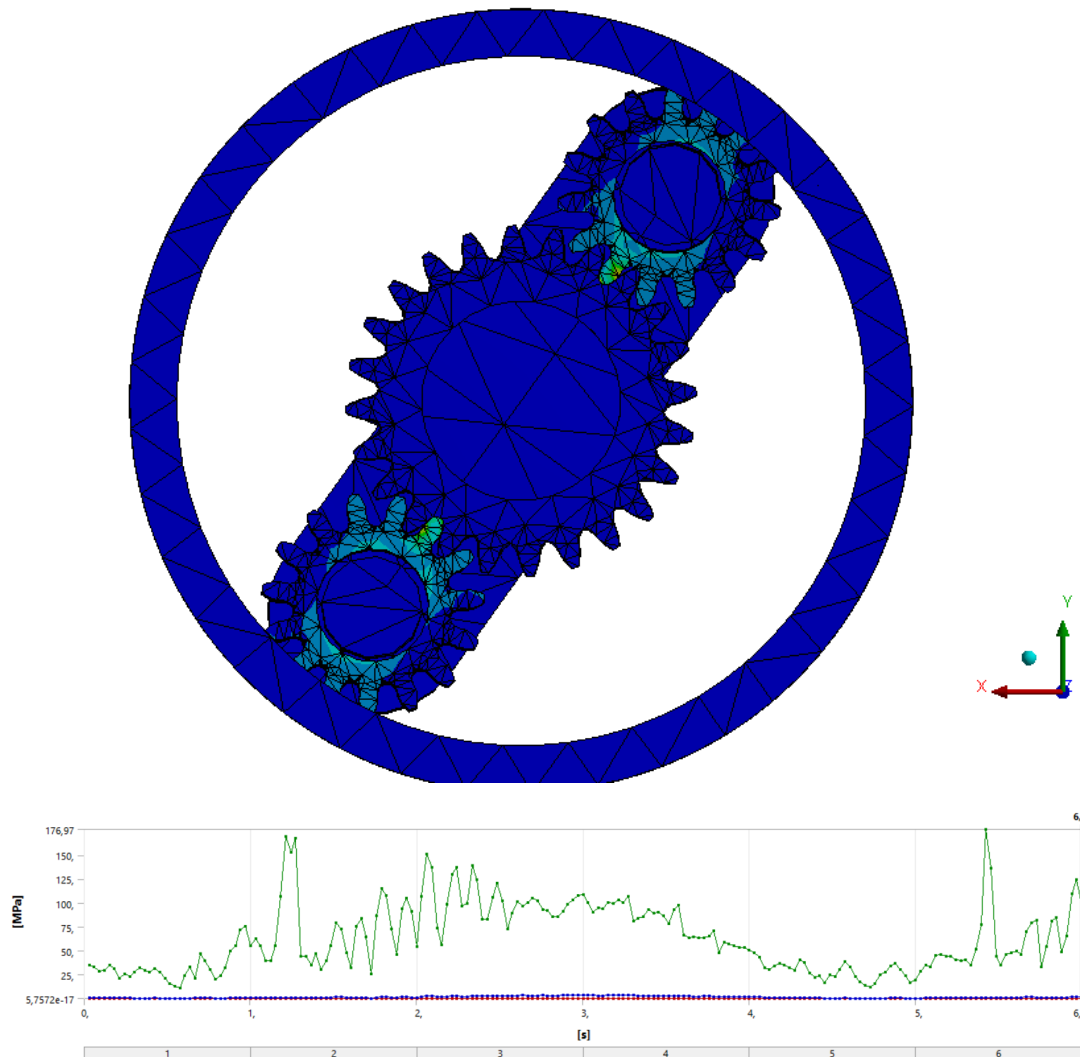
The transient analysis of the PGT system was done using the given profile as it could replicate better the problem. The analysis was using the two different profiles and what are their effects on the teeth and the efficiency of the system.

The transient analysis that was conducted on the PGT had as a purpose to show the effect of misalignments on the gears with the carrier, as well as the counter moments and forces that were produced by the rollers effecting the transmission of the gears.

The gears were able to move freely along the XY plane and had a forced  $2^\circ$  misalignment as explained before. Due to effect of the misalignment and the rotation the planets were either with close contact with the sun or with the ring and according to each contact the stresses.

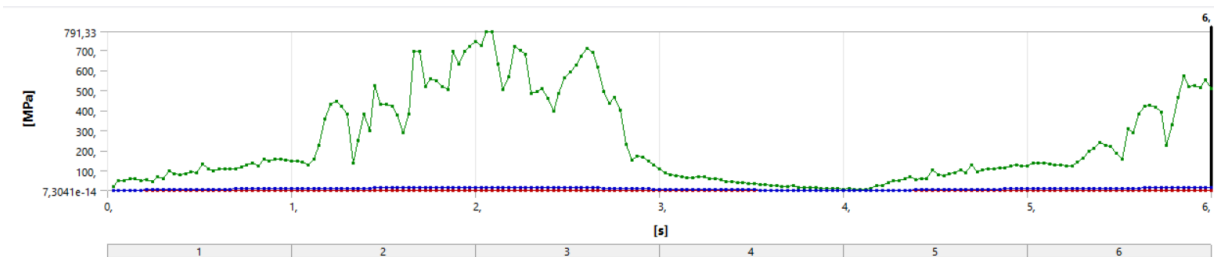
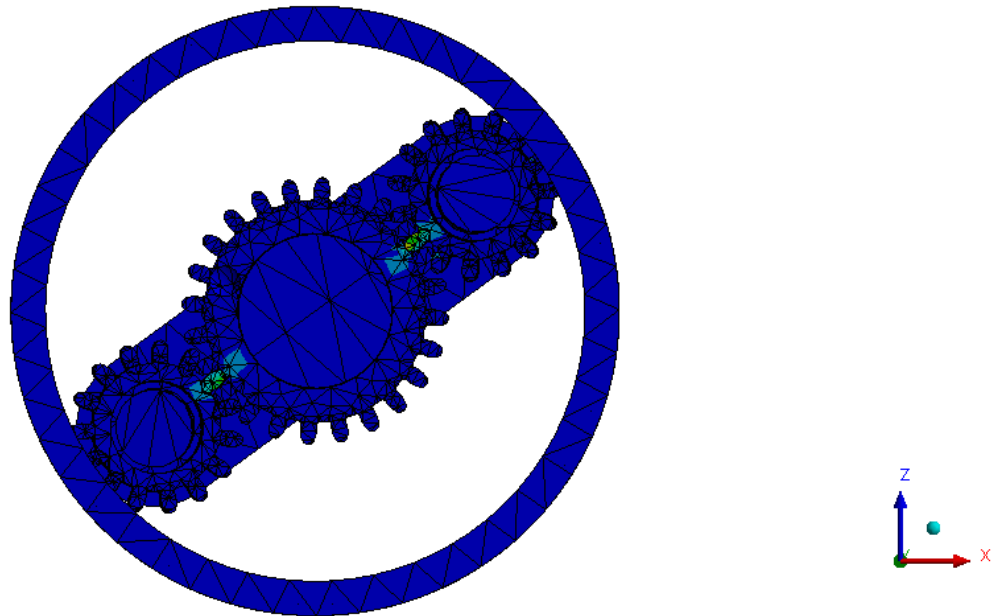
#### 5.1.6.1 Modified Involute Profiles

The modified profiles showed a better behavior when tested in the transient analysis in the presence of misalignments, with minimum Equivalent Stresses, as expected.



### 5.1.6.2 Given Profiles

The given profile performed worse vis a vis the Equivalent Stress applied on the faces of the gears during the rotation. In the long run this could damage the teeth reducing the life of the product as well as reducing the efficiency of the system overall.



## 5.2 Analysis of the RPC system

### 5.2.1 Transient Analysis of the Roller-pump-carrier system

The model of the rollers with the carrier and the tube was the most crucial model as it could show both the effects of the misalignments on the contact surfaces of the rollers, as well as the deformation of the tube. However due to computational limitations and the complexity of the model it was decoupled.

The RPC system consists of the roller-pump-carrier without the gears meshing. Three tests were done on the model, one with loose fit one with a tight fit and one with a tight fit and deep occlusion.

#### 5.2.1.1 RPC with tight fit

The tight fit model caused more elastic strain on the tube, as expected because the rollers did not have any room to move, therefore they acted more as solid body. However, the energy required to move it and to compress the tube is greater than the one in the tight fit as seen in figure 48. This also verifies the experimental results of another study

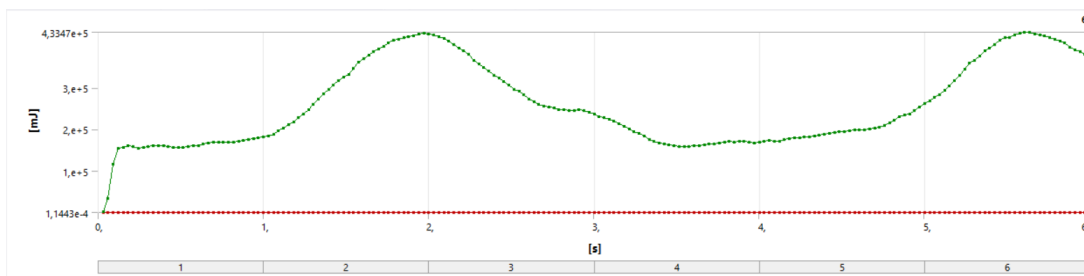


Figure 48 Energy consumption for tight fit

#### 5.2.1.2 RPC with loose fit

The transient analysis of the loose fit, even though it yielded worst results regarding the compression of the tube and therefore the flow rate, also it required less energy.

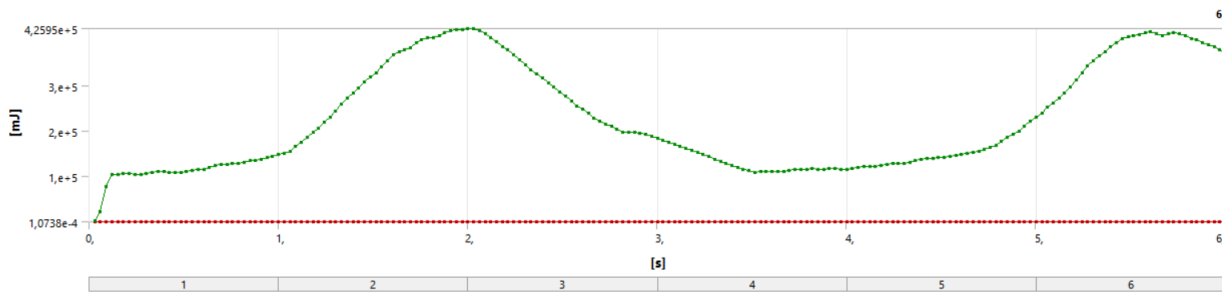
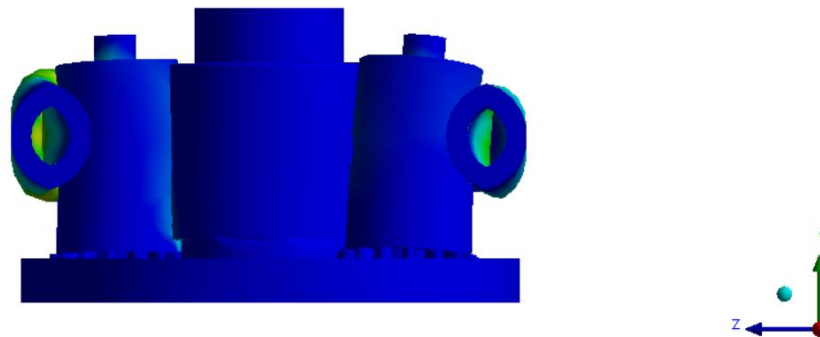


Figure 49 Energy consumption for loose fit

However, it was able to capture more accurately the real model, as the rollers can be seen in figure 50 having great misalignments due to the compression of the tube as well as the compression on the roller of the sun.



*Figure 50 Rollers movement*

#### *5.2.1.3 RPC deep occlusion*

The deep occlusion model with the tight fit had the biggest elastic strain as expected

**B: Transient Structural**  
 Equivalent Elastic Strain  
 Type: Equivalent Elastic Strain  
 Unit: mm/mm  
 Time: 3,7695  
 Max: 0,58494  
 Min: 6,3813e-9  
 24/10/2022 7:17 πμ

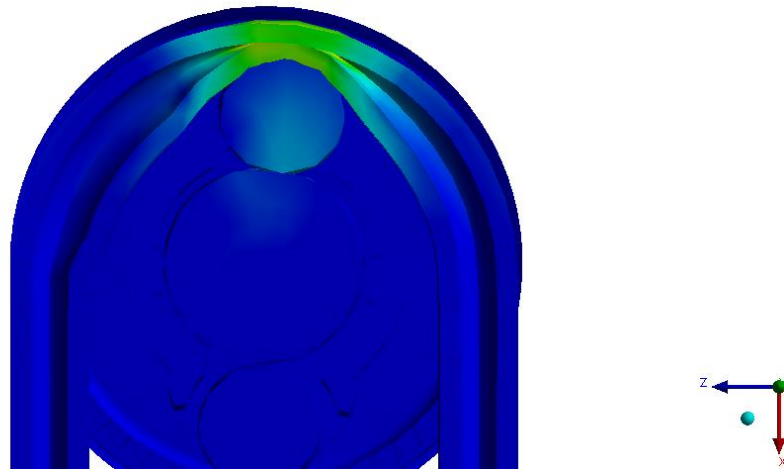


Figure 51 Elastic Strain of deep occlusion

Moreover, it was the most energy consuming of the three tests. This can be explained because the energy required to fully compress the tube as well as the frictional forces that develop between the tube and the rollers are far greater than in the other two analyses.

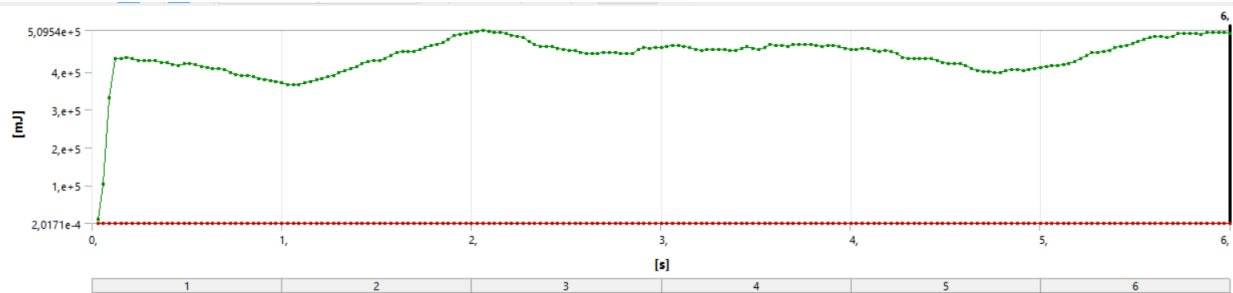


Figure 52 Energy consumption of deep occlusion

Therefore, this model requires the most energy but would yield the best results regarding the flow rate.

## 6. Conclusion

The goal of this thesis was to give a deeper understanding of the phenomena that govern this mechanism as well as a more complete image of the modelling that was needed to be done in order to compare experimental results with the theoretical data of the FEM analysis. In particular, the most studied phenomenon was that of the misalignments in a one-stage gear transmission as well as in the PGT. From those FEM analysis it was concluded that the involute profile while better at handling loads in the planar tests, even with a small misalignment of  $2^\circ$  it showed an increase in contact pressures of up eightfold comparing to the modified profiles that showed no significant change. Furthermore, the given profiles while comparing to the modified profiles when misaligned had a very low degree of overlap comparably to the other two. When Moreover, after the testing in static analysis of a gear pair of the modified and the given profiles. It was deemed necessary to compare both profiles in a transient analysis as a PGT because of the application and they were tested to see the results that yielded. As mentioned, the modified profile showed better behavior and overall.

Furthermore, the RPC system was found to be greatly influenced by the misalignments cause by the compression of the tube and by the fits that it had. When applied with a tighter fit it, while requiring greater energy input due to the power losses in friction it showed better control of the compression of the tube and therefore of the flow rate.

Therefore, there is great merit in a study of the whole system using the newly required data from the previous analysis. Also, it could be interesting to see the results of both profiles when put into testing in order to both evaluate the fittings of the planets as well as the profiles. However, it should be noted that a new design at certain part of the pump is required, the support of the sun that is attached to the ring should be improved to reduce friction as well as increase stability. The fittings on the carrier should, also, be designed as cylindrical surfaces or at least a part of a cylinder so that it is more feasible to predict the motion of the rollers as well as the modelling in FEM analysis.

Finally, the model with tighter fittings had a better behavior when compressing the tube however, it also requires greater amounts of energy, due to frictional forces. Therefore, it is deemed necessary to use the models developed in this thesis to acquire more information regarding the flow rate and the power loss of the pump and PGT altogether.

## 7. References

- [1] K. József and K. Levente, "A review on working and control possibilities".
- [2] G. Ramalingam and S. Subramaniam, "MODELING AND CONTACT ANALYSIS OF CROWNED SPUR GEAR TEETH," *Engineering MECHANICS*, vol. Vol. 18, no. 1, pp. 65-78, 2011.
- [3] E. Jason, K. Saravanan and P. Santosh, "Frictional stress analysis of spur gear with misalignments," *Journal of Mechanical Engineering and Sciences*.
- [4] B. Grzegorz, M. Tadeusz, B. Michal, J. PISULA, J. PACANA and B. KOZIK, "STRESS ASSESSMENT OF GEAR TEETH IN EPICYCLIC GEAR TRAIN FOR RADIAL SEDIMENTATION TANK," *sciendo*, vol. 14, no. 3, p. 7, 2020.
- [5] J. Martin, "Planetary Gear Analysis – deformation induced misalignment and optimization," Stockholm, 2020.
- [6] Κ. Θ., *Οδοντώσεις και Μειωτήρες Στροφών.*, Αθήνα: Εκδόσεις Συμείων, 2010.
- [7] M. Obermayr, "A six parameter Shell Element for Linear Static Analysis," Braunschweig, 2004.
- [8] S. Senthivelan and R. Gnanamoorthy, «Damage mechanisms in injection molded reinforced, glass.
- [9] Rajesh, "Design and Contact Analysis of Plastic Spur Gears," *IJARTET*, vol. 3, no. 19, p. 6, 2016.